npg

ORIGINAL ARTICLE

Depletion of STAT5 blocks TEL–SYK-induced APMF-type leukemia with myelofibrosis and myelodysplasia in mice

C Sprissler[1,2,6], D Belenki[1,6], H Maurer[1,6], K Aumann[3], D Pfeifer[1], C Klein[1], TA Müller[1], S Kissel[1], J Hülsdünker[1], J Alexandrovski[1], T Brummer[4,5], H Jumaa[3,4,5], J Duyster[1] and C Dierks[1,5]

The spleen tyrosine kinase (SYK) was identified as an oncogenic driver in a broad spectrum of hematologic malignancies. The *in vivo* comparison of three SYK containing oncogenes, SYK[wt], TEL–SYK and IL-2-inducible T-cell kinase (ITK)-SYK revealed a general myeloexpansion and the establishment of three different hematologic (pre)diseases. SYK[wt] enhanced the myeloid and T-cell compartment, without leukemia/lymphoma development. ITK–SYK caused lethal T-cell lymphomas and the cytoplasmic TEL–SYK fusion induced an acute panmyelosis with myelofibrosis-type acute myeloid leukemia (AML) with up to 50% immature megakaryoblasts infiltrating bone marrow, spleen and liver, additional MPN features (myelofibrosis and granulocyte expansion) and MDS stigmata with megakaryocytic and erythroid dysplasia. LKS cells were reduced and all subsets (LT/ST/MPP) showed reduced proliferation rates. SYK inhibitor treatment (R788) of diseased TEL–SYK mice reduced leukocytosis, spleen and liver infiltration, enhanced the hematocrit and prolonged survival time, but could not significantly reduce myelofibrosis. Stat5 was identified as a major downstream mediator of TEL–SYK *in vitro* as well as *in vivo*. Consequently, targeted deletion of *Stat5 in vivo* completely abrogated TEL–SYK-induced AML and myelofibrosis development, proving Stat5 as a major driver of SYK-induced transformation. Our experiments highlight the important role of SYK in AML and myelofibrosis and prove SYK and STAT5 inhibitors as potent treatment options for those diseases.

Blood Cancer Journal (2014) **4**, e240; doi:10.1038/bcj.2014.53; published online 22 August 2014

INTRODUCTION

Constitutive activation of tyrosine kinases either by fusion of the kinase domain to dimerizing proteins or by point mutations inducing constitutive activation are a broadly accepted cause for cancer development. One player, the spleen tyrosine kinase (SYK) was shown to be involved in propagation of several hematologic malignancies.

SYK[wt] is expressed in most hematopoietic cells[1–4] and is involved in Fcγ receptor signaling,[5] B- and T-cell antigen receptor signaling,[6–8] immunoglobulin E receptor signaling,[9] several interleukin receptors[10–12] and integrins like αIIb/β3.[5,13,14] SYK belongs to the SYK/ZAP-70 family of non-receptor tyrosine kinases.[15,16] Without receptor stimulation, SYK is autoinhibited and exists in a closed conformation. Upon activation of immunoreceptors, SYK becomes phosphorylated by SRC family kinases and binds to immunoreceptor tyrosine-based activation motifs mediated by its two tandem SH2 domains.[8,17,18] SYK activation induces phosphorylation of SLP65, SLP76, PLCγ1/2 and VAV, resulting in activation of the phosphatidylinositol 3-kinase pathway, calcium ion signaling and mitogen-activated protein kinase signaling.[19–25]

Overexpression and activation of SYK[wt] was identified in various B-cell lymphoma subtypes.[26–28] In chronic lymphocytic leukemia,[29] SYK functions as a downstream signaling mediator of the autoreactive B-cell receptor[30] and propagates microenvironment driven chemokine receptor signaling like CXCR4.[13]

In acute myeloid leukemia (AML) cells, constitutive activation of SYK occurs independent from the driving oncogene, but depends on tonic activation of the Fc-γR1 and Mac-1 receptors, stimulated by cytokines delivered from the bone marrow (BM) niche.[5,31] Beside constitutive activation of SYK through upstream signaling events, two fusion oncogenes, interleukin-2 (IL-2)-inducible T-cell kinase (ITK)-SYK and TEL–SYK contain the constitutively activated tyrosine kinase domain of SYK.

ITK–SYK arises from a fusion between SYK and the ITK. It has been identified as a recurrent translocation in 17% of patients with unspecified peripheral T-cell lymphomas.[32] The highly aggressive disease is characterized by infiltration of skin, spleen, lymph nodes, BM and other organs with mature T cells. The ITK-part of the ITK–SYK fusion contains a Pleckstrin-homology domain targeting the protein to the plasma membrane, and a Tec-homology domain, which is linked to the tyrosine kinase domain of SYK. Previously, we and others could show that expression of ITK–SYK in murine BM or CD4+ cells leads to T-cell lymphoma development in mice, reflecting all major characteristics from the human disease.[33,34]

TEL–SYK was identified in a patient with an atypical myelodysplastic syndrome with leukemic transformation.[35] The patient was characterized by refractory anemia, dysplasia of the megakaryocytic and erythroid lineage, as well as myeloid hyperplasia with excess blasts (RAEB-T) with megakaryocytic phenotype. The patient progressed to leukemia with CD41+ megakaryocytic blasts.[35]

[1]Department of Hematology/Oncology, University Medical Center Freiburg, Freiburg, Germany; [2]University of Freiburg, Schaenzlestrasse 1, Freiburg, Germany; [3]Department of Pathology, University Medical Center Freiburg, Freiburg, Germany; [4]Institut für Molekulare Medizin und Zellforschung, University of Freiburg, Stefan-Meier-Str. 17, Freiburg, Germany and [5]Centre for Biological Signaling Studies BIOSS, Freiburg, Germany. Correspondence: Dr C Dierks, Department of Hematology/Oncology, University Medical Center Freiburg, Hugstetter Strasse 55, 79106 Freiburg, Germany.
E-mail: christine.dierks@uniklinik-freiburg.de
[6]These authors contributed equally to this study.

2

In TEL–SYK, the E26 transforming-specific translocation variant gene 6 (*ETV6*) is fused to the C-terminal part of SYK containing the tyrosine kinase domain and the Interdomain B. Although ITK–SYK is mainly localized in lipid rafts at the cell membrane, TEL–SYK has a cytoplasmic localization[34,36] and is constitutively activated through TEL-mediated oligomerization.[37] Overexpression of the TEL–SYK fusion in murine pre B cells induces a B-ALL like disease in mice.[38] Furthermore, the expression of TEL–SYK in fetal liver cells was shown to induce myelofibrosis and myelodysplasia in transplanted mice.[39]

Given those previously published papers, SYK overexpression as well as constitutive activation by fusions or other activating mechanisms seems to be a general theme for many different hematologic malignancies. On the other hand, the SYK fusion partners, the activation mechanism and the fusion partner-dependent localization of the fusion protein seem to have a pivotal role in selecting the transformed population. Therefore, the aim of the study was to compare the transformation potential of the known oncogenic SYK fusions and SYK[wt] *in vivo*, to precisely monitor their diverging influence on different hematologic cell subsets and to identify the underlying cell context dependent signaling events with focus on signal transducers and activators of transcription (STAT) signaling.

MATERIALS AND METHODS

Mouse experiments

All animal experiments were conducted in compliance with the US department of Health and Human Service Guide for Care and Use of Laboratory Animals and in concordance with German law. Experiments were approved by the Regierungspräsidium Freiburg. BALB/c or C57BL/6 males were injected intraperitoneally with 5-fluorouracil (150 mg/kg) and were killed after 4 days. Bone marrow cells (BMCs) were harvested, followed by erythrocyte lysis (Qiagen, Hilden, Germany) and cultivated for 2 days in prestimulation medium with DMEM (Gibco, New York, NY, USA) with 10% FBS (Biochrom, Berlin, Germany), mSCF, mIL-6 and mIL-3 (Peprotech, Hamburg, Germany) before transplantation. BMCs were transduced twice with retroviral particles generated by HEK293T, which had been transfected with pMSCV/ IRES/ green fluorescent protein (GFP; pMIG) empty control vector or vector with integrated SYK[wt], ITK-SYK and TEL–SYK together with an EcoPack packaging vector (BD Bioscience, Heidelberg, Germany). Infection efficiency in different cell subsets was assessed 24 h after the 2nd infection round. BMCs (6×10^5) expressing the different oncogenes were transplanted via retroorbital injection into sublethally irradiated recipient BALB/c or C57BL/6 females (2×450 cGy). Disease development was monitored by inspection for general disease symptoms (mobility, hunched back, rough fur), weight measurements, biweekly blood cell counts (ADVIA120 Analyzer, Siemens, Munich, Germany) and flow cytometry analysis of peripheral blood cells for B cells (B220), T cells (CD3, CD4, CD8), myeloid cells (CD11b/Gr-1) and blasts (cKit).

Mice were killed when moribund and BM, spleen, liver, lymph nodes and other organs were extracted for weight comparison (spleen and liver) and for evaluation of total cell numbers (femurs and spleens). Organs were fixed in formalin for immunohistochemistry or directly analyzed by flow cytometry (Beckmann Coulter, Krefeld, Germany).

For the retransplantation experiment, BMCs or spleen cells of diseased TEL–SYK mice (2×10^6 GFP-positive cells) were added to 6×10^6 normal BMCs and transplanted into irradiated recipient BALB/c females. The control group obtained 6×10^6 control BMCs.

Deletion of Stat5 *in vivo* was performed with *Stat5^{fl/fl}Mx1Cre* BMCs. The original *Stat5[fl/f]* mouse strain was developed by L Hennighausen[40] and the *Stat5^{fl/fl}Mx1Cre* has previously been described.[41] *Stat5^{fl/fl}Mx1Cre* or *Stat5^{fl/fl}* (as control) BMCs were retrovirally transduced with TEL–SYK as described above and retroorbitally transplanted into twice irradiated recipient Balb/c females (2×450 cGy). The *Stat5a/b* locus was excised by three times intraperitoneally injection of 250 μg Poly (I:C) every 4 days starting d7 (see Hoelbl *et al.* (2010)).[41]

For SYK inhibitor treatment studies, 2 weeks after transplantation, mice were split into two similar groups (seven to eight mice per group) according to the GFP content in the peripheral blood and body weight. One group was treated via oral gavage twice a day with 40 mg/kg R788 (Shanghai Haoyuan Chemexpress, Shanghai, China), solved in 0.1% carboxymethylcellulose sodium, 0.1% methylparaben, 0.02% propylparaben (Sigma-Aldrich, Munich, Germany) for 21 days and the other group with vehicle.

Plasmids

The pMSCV/IRES/GFP (pMIG) vector,[42] ITK–SYK[33] and TEL–SYK[38] constructs were described previously. The HuSYK[wt] pENTR(tm)221 vector was purchased from ImaGenes (Berlin, Germany) and SYK[wt] was cloned into a gateway-adapted pMIG vector via homologous recombination (Invitrogen).

Cell culture

293T cells were cultured in DMEM medium (Gibco) supplemented with 10% fetal bovine serum (PAA Laboratories, Pasching, Austria) and 1% penicillin–streptomycin (Gibco). BaF3 and 32D cells were obtained from ATCC and cultivated in RPMI-1640 medium (Gibco) with 10% fetal bovine serum, 1% penicillin–streptomycin and 10% WEHI supernatant. For phosphorylation experiments (phospho-flow or western blots), cells were cultivated without IL-3 for 15 h. Human KG-1 AML cells (erythroid leukemia, ATCC) and SET-2 cells (JAK2V617F+ megakaryoblastic leukemia, DSMZ) were cultured in RPMI-1640 medium with 10% or 20% FBS, respectively.

### Proliferation and apoptosis assays

For SYK inhibition, the SYK inhibitor R406 (Axon medchem, Genentech, San Francisco, CA, USA) was solved in dimethylsulfoxide and used at a final concentration of 2 and 4 μM. For STAT5-inhibition pimozide (Calbiochem, San Diego, CA, USA) was solved in dimethylsulfoxide and used at a final concentration of 5 and 10 μM. 32D cells supplemented with IL-3, 32D TEL–SYK cells without IL-3, 32D BCR–ABL cells without IL-3, KG-1 cells and

Figure 1. TEL–SYK induces a leukemic disease with anemia and thrombocytopenia in mice. (**a**) Schematic representations of SYK[wt], ITK–SYKSYK and TEL–SYK. PH, pleckstrin-homology domain; PNT, pointed N terminal domain; SH2, Src homology 2 domain; TK, tyrosine kinase domain; TH, Tec-homology domain. (**b**) Kaplan–Meier survival curve representing the survival of Balb/c mice either transplanted with control BM (empty pMSCV/IRES/GFP vector), SYK[wt], ITK–SYK or TEL–SYK BM ($n = 8$ per group). TEL–SYK mice died after 21–28 days, whereas ITK–SYK mice survived 42–76 days. Control and SYK[wt] mice were killed after 200 days without any disease symptoms. (**c**) Mean spleen weights of control, SYK[wt], ITK–SYKSYK and TEL–SYK-transplanted Balb/c mice 25 and 42 days post transplantation. ITK–SYKSYK and TEL–SYK mice develop a splenomegaly with an approximately fourfold increase in spleen weights for TEL–SYK mice after 25 days and a twofold increase for ITK–SYK mice after 42 days (left panel) (*$P < 0.05$; **$P < 0.01$; ***$P < 0.001$; unpaired *t*-test). (**d**) Peripheral blood samples of control, SYK[wt], ITK–SYKSYK and TEL–SYK mice were analyzed for red blood cell counts, hematocrit, WBC counts and thrombocytes 25 and 42 days post transplantation with the ADVIA120 blood analyzer (control 25d $n = 7$, SYK $n = 5$, ITK–SYK $n = 6$, TEL–SYK $n = 7$) *$P < 0.05$; **$P < 0.01$; ***$P < 0.001$, unpaired *t*-test. (**e**) May-Grünwald/Giemsa stain of blood smears of mice expressing control vector, SYK[wt], ITK–SYK or TEL–SYK 25 days post transplantation. TEL–SYK mice show a strong expansion of differentiated granulocytes and megakaryoblasts in the peripheral blood. Bars, 50 μm. (**f**) Differential blood analysis from blood smears from the different transplantation groups ($n = 4$ mice per group) 25 days after transplantation. Graph represents the percentage of neutrophils, lymphocytes, bands, monocytes, eosinophils and blasts within total leukocytes and is given as mean+s.e.m. (**g**) Flow cytometry analysis for CD11b (myeloid cells), B220 (B cells) and CD90/CD3 (T cells) in the peripheral blood of the different transplantation groups analyzed in **d**. Bars represent the mean percentage+s.e.m of CD11b+ cells, B220+ cells and CD90+/CD3+ cells within the GFP+ (black border) and the GFP- (gray border) population, to allow discrimination of oncogene-driven cell intrinsic and cell extrinsic effects. GFP+ cells represent the cells carrying the respective oncogene or the control vector. (control $n = 6$, SYK 25 days $n = 6$, SYK 42 days $n = 5$, TEL–SYK $n = 7$, ITK–SYK $n = 7$) *$P < 0.05$ **$P < 0.01$; ***$P < 0.001$, unpaired t-test. ** above the white bars represents the significance of the difference between the GFP+ and GFP- population within the same mice.

SET-2 cells were treated as indicated and cell numbers were assessed by Trypan blue staining and counting via Neubauer chamber for 24–72 h. For apoptosis detection after 48 h treatment, cells were stained with AnnexinV-APC/7-AAD (BD Pharmingen, Uppsala, Sweden) according to the manufacturer's instructions and measured by flow cytometry.

Flow cytometry

Surface staining of BMC and spleen cells previously treated with erythrocyte lysis buffer (Qiagen) was performed with antibodies from BD Pharmingen against CD3-PE-Cy7, CD4-APC, CD8-PB, B220-APC, Ter119-PE-Cy7, CD11b-PE-Cy7, CD19-PE-Cy7, Gr-1-PE-Cy7, Gr-1-PB and
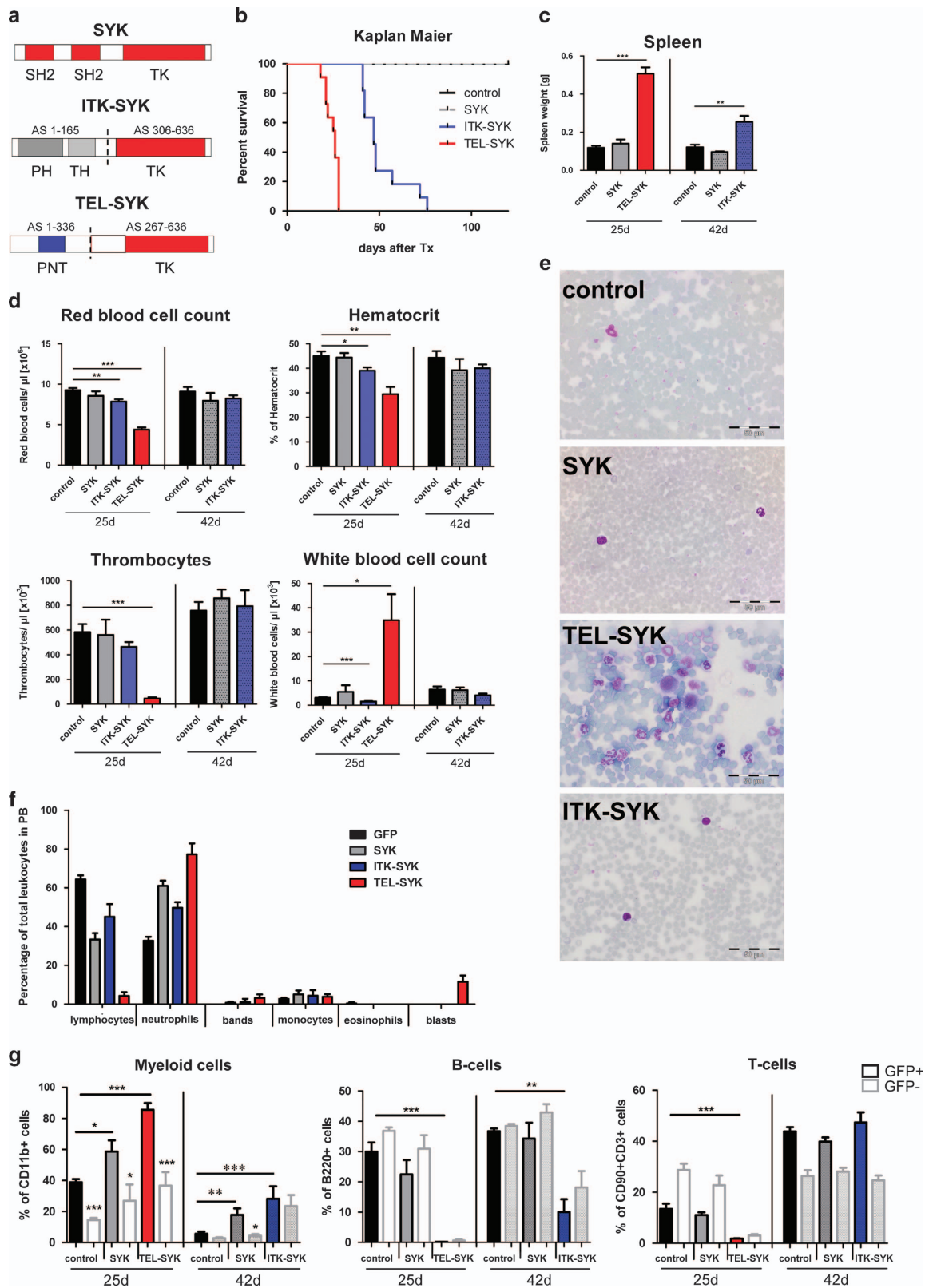
Sca1-PB; cKit-APC from BioLegend (San Diego, CA, USA), and CD90.2-PE-Cy7 from eBioscience (San Diego, CA, USA) and measured using the CyanADP flow cytometer (Beckmann Coulter). Flow cytometry data were analyzed using the FlowJo 7.6 software (Tree Star, Inc., Ashland, OR, USA).

Intracellular phospho flow cytometry

For intracellular phospho flow cytometry, spleens of SYK[wt], TEL–SYK, ITK–SYK or control mice were harvested, passed through a 100-μm filter (Millipore, Billerica, MA, USA) and directly fixed in 2% formaldehyde,
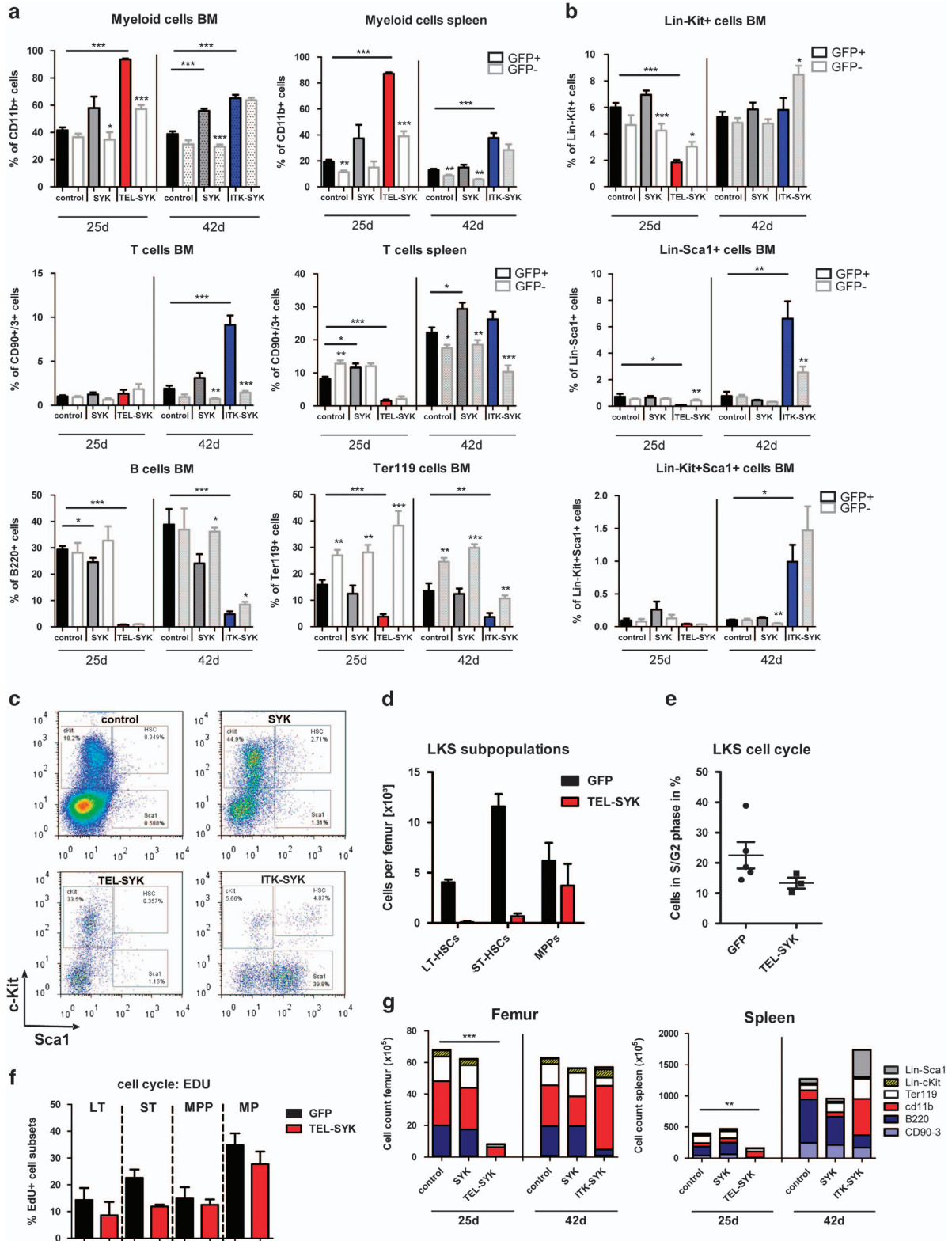
followed by 30 min permeabilization with 90% methanol. Then cells were stained with APC-labeled antibodies against phospho-STAT5 pY694, phospho-STAT6 pY641, phospho-PLCγ1 pY783, phospho-PLCγ2 pY759 and phospho-SLP76 pY128 (all BD Phosflow) for 1 h and measured using the CyanADP flow cytometer (Beckmann Coulter).

Phosphorylation analysis after R406 (Axon medchem) treatment of 32D TEL–SYK cells (depleted of IL-3), KG-1 cells and SET-2 cells was performed after 5 min, 30 min and 2 h.

Western blot

Western blots were performed using standard methods using a Reinhard lysis buffer supplemented with protease and phosphatase inhibitors (Roche, Basel, Switzerland). For phosphorylation studies, BaF3 and 32D cells were depleted of IL-3 for 15 h. Proteins were blotted on a nitrocellulose membrane. Primary antibodies were used at 1:1000 in 1% milk over night at 4 °C against phosphorylated and non-phosphorylated STAT1 (pY701), STAT3 (pY705 and pS727), STAT5 (pY694), STAT6 (pY641), JAK2, PLCγ1 (pY783), PLCγ2 (pY759), SLP76, ERK (T202/Y204), AKT (S473), SYK, ITK (all Cell Signaling, Danvers, MA, USA), JAK2, TEL (Santa Cruz Biotech, Dallas, TX, USA), SLP76 (pY128) (BD Pharmingen), and β-Actin (Sigma-Aldrich). Secondary HRP-labeled antibodies (Cell Signaling Technology) were used at 1:2500. Membranes were incubated with ECL (Amersham, London, UK) for 2 min and chemiluminescence was detected using a western blot detection system (Curix 60, AGFA).

Immunohistochemistry staining

Paraffin-embedded spleen, liver and BM sections were acquired from the pathology department of the University of Freiburg and stained for hematoxylin/eosin, periodic acid–Schiff stain and reticulin following standard procedures. Blood smears were stained with May-Grünwald–Giemsa. Histology slides were analyzed by a pathologist from the Medical University Freiburg. Images were taken with the LCmicro from Olympus.

Cell cycle analysis

TEL–SYK mice and GFP-control mice were injected with 100 μl/20 g body weight of 10 mM EdU (Click-iT EdU Pacific Blue Flow Cytometry Assay Kit, Molecular Probes, Eugene, OR, USA). BMCs were harvested 15 h later and LT-HSCs (Lin − cKit+Sca1+CD135 − CD150+), ST-HSCs (Lin − cKit+Sca1 +CD135 − CD150 −), MPPs (Lin − cKit+Sca1+CD135+CD150 −) and myeloid progenitors (MPs) (Lin − cKit+Sca1 −) were sorted with the ARIA III cell sorter (BD Biosciences). Samples were prepared according to the manufacturer's instructions and were analyzed for EdU+ cells by flow cytometry (Beckman Coulter). For cell cycle analysis of LKS cells in the BM, we used FxCycle^T Violet stain (Molecular Probes) to stain DNA in combination with Lin(CD11b/Gr-1/CD3/CD19/Ter119)-PeCy7, cKit-APC, Sca1-APCCy7, CD135-PECy5 and CD150-PE (Biolegend) antibodies.

Gene arrays

TEL–SYK and GFP-control LT/ST-HSCs were pooled from three to four mice and sorted as described above. RNA from LT and ST-HSCs was extracted with the RNeasy Micro Kit (Qiagen). RNA integrity was analyzed by capillary electrophoresis using a Fragment Analyser (Advanced Analytical Technologies, Heidelberg, Germany). RNA samples had an RNA quality number of

greater than 8.7 and were further processed with the NuGEN Ovation Pico WTA V2 kit (NuGEN, Cumbria, UK) as described by the manufacturer. NuGEN whole transcriptome amplified TEL–SYK and control LT-HSC samples were technical replicates from the same RNA. The NuGEN assay amplification yielded more than 5.5 μg of cDNA from 2 to 10 ng of total RNA. The amplified cDNA was further fragmented and labeled using the Affymetrix WT Terminal labeling and control kit. Labeled fragments were hybridized to GeneChip Mouse Gene ST 2.0 arrays for 16 h at 45 °C with 60 r.p.m. in an Affymetrix Hybridization oven 640. After washing and staining, the arrays were scanned with the Affymetrix GeneChip Scanner 3000 7 G. CEL files were produced from the raw data with Affymetrix GeneChip Command Console Software Version 4.0. We used Partek Genomics Suite software for further analysis (Partek, Inc., Görlitz, Germany). Here, CEL files were imported including control and interrogating probes.

Prebackground adjustment was set to adjust for GC Content and probe sequence and RMA background correction was performed. Arrays were normalized using Quantile normalization and probeset summarization was done using Median Polish. Probe values were log2 transformed.

In order to identify differentially expressed genes between the groups, we performed a one-way analysis of variance in Partek. Using Fisher's Least Significant Difference as contrast method, the following contrasts were performed to compare: LT-TEL–SYK versus LT-GFP, ST-TEL–SYK versus ST-GFP, LT-TEL–SYK versus ST-TEL–SYK, LT-GFP versus ST-GFP.

Transcript cluster IDs were filtered for annotation categories main, rescue and reporter, such omitting control probes from further analysis. Hierarchical clustering was performed using Partek Genomics Suite.

Gene set enrichment analysis was performed by using the KEGG gene set database as described previously.[43] Threshold for significance was set to a nominal P-value < 0.05, normalized enrichment score >1.5 or < − 1.5 and false discovery rate < 0.25.

Statistical analysis

Data are represented as mean ± s.e.m. Significance between parameters were analyzed with a two-tailed, paired or unpaired Student's t-test or Mann–Whitney test. For all analyses, P < 0.05 was considered statistically significant.

RESULTS

ITK–SYK and TEL–SYK, but not SYK^{wt} cause a lethal hematologic disease in mice

To investigate differences of SYK^{wt}, ITK-SYK and TEL–SYK on hematopoiesis development and transformation, the oncogenes were cloned into a retroviral vector (pMSCV/IRES/GFP = pMIG; Figure 1a, composition of SYK^{wt} and SYK fusion domains), expressed in 5-Fluorouracil-pretreated BM and BM cells were then transplanted into sublethally irradiated Balb/c recipients. BM infection rates measured by GFP content 48 h after infection were in between 25 and 50% for all constructs and infection of different cell subsets (B cells, T cells, myeloid cells, HSCs) was equal in between the different groups and as previously described.[33]

The three SYK oncogenes caused remarkable differences in disease development. Three weeks after transplantation, TEL–SYK

Figure 2. SYK oncogenes drive myeloid and T-cell expansion and alter the HSC pool. (**a**) BM and spleen cells of control, ITK–SYK, TEL–SYK and SYK^{wt} mice (n = 7–8) were analyzed by flow cytometry for expression of CD11b/Gr-1 (myeloid cells), CD90/CD3 (T cells), B220 (B cells) and Ter119 (erythroid progenitors) within the oncogene carrying GFP+ and the GFP − population representing normal hematopoiesis within the same mouse. Bars represent the mean percentage within live cells+s.e.m. (**b**) Analysis of same samples for myeloid progenitors (Lin-Kit +Sca1 −), lymphoid progenitors/mesenchymal stem cells (Lin − Kit-Sca+) and hematopoietic stem cells (Lin − Kit+Sca1+). Bars represent the mean percentage within live cells+s.e.m. (**c**) Flow cytometry analysis of Lin − cells (gated in control mice to present 10–12% of the total live gate). Gates were kept for all other transplantation groups. Shown is the Kit/Sca1 staining of one representative example per group. (**d**) Graph shows total numbers of LKS subpopulations (LT-HSCs, ST-HSCs, MPPs) as assessed by flow cytometry and calculated per femur in C57BL/6 mice. (**e**) Graph shows the percentage of LKS cells in S/G2 phase as assessed by FxViolet DNA staining in Balb/c mice. (**f**) EdU labeling of TEL–SYK mice versus control mice for 15 h. Graph shows numbers of EdU+ cells within the different LKS subpopulations and myeloid progenitors. LT are defined as Lin − Kit+Sca+CD150+FLT3 − cells, ST as Lin − Kit+Sca+CD150-FLT3 − cells, MPP as Lin − Kit+Sca+CD150 − FLT3+ cells and MPs as Lin − Kit+Sca − cells. (**g**) Total cell numbers per femur and per spleen were counted for each mouse used in **a**. Bars represent the mean total cell number per transplantation group and shows the distribution of the different cell types within this groups. *P < 0.05; **P < 0.01; ***P < 0.001, unpaired t-test. **above the white bars represents the significance of the difference between the GFP+ and GFP − population within the same mice.
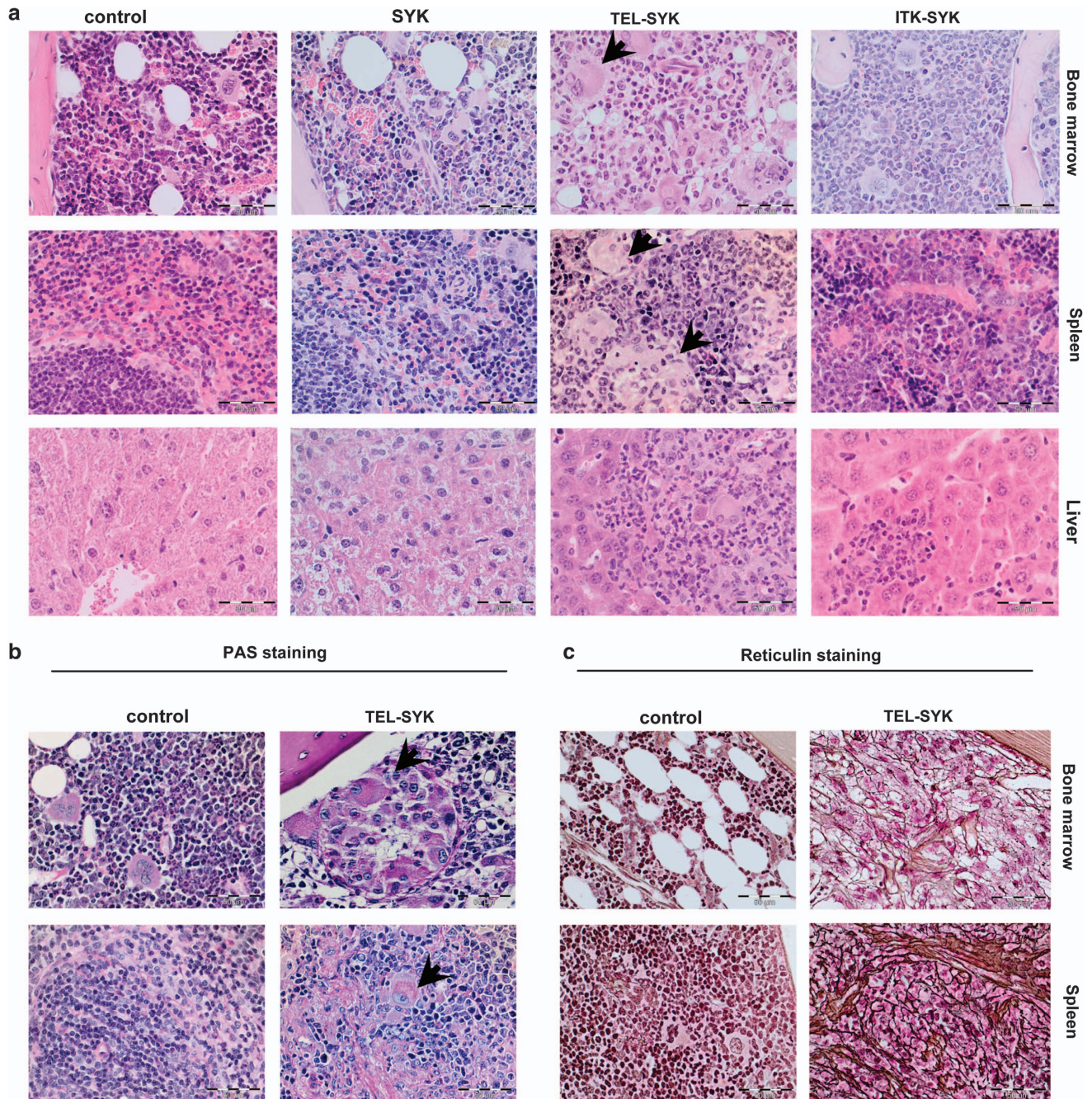
Figure 3. TEL–SYK induces an AML with features of human APMF in mice. (**a**) Images from hematoxylin and eosin-stained BM, spleen and liver slides from control, SYK^wt, TEL–SYK and ITK–SYK mice. ◄shows dysplastic and immature megakaryocytes /megakaryoblasts infiltrating BM, spleens and the liver of TEL–SYK mice. Bars, 50 μm. (**b**) Periodic acid–Schiff (PAS) stain of BM and spleens from control and TEL–SYK mice highlight the infiltrating megakaryoblasts in TEL–SYK mice. (**c**) Reticulin stain of BM and spleens of diseased TEL–SYK mice compared with controls display a strong fibrosis (II–III) in both organs (right panel). Bars, 50 μm.

mice developed general disease symptoms (weight loss of more than 20%, reduced mobility, rough fur) and all mice in that group ($n = 8$) had to be killed due to final disease within 28 days after transplantation (Figure 1b). ITK-SYK-transplanted mice also developed a lethal disease, but had nearly twice as long survival time of 41–76 days. SYK^wt, as well as GFP-control mice did not show any signs of disease until 200 days after transplantation (Figure 1b).

Analysis of spleens and livers at the time of death revealed a significant fourfold increase in spleen weights for TEL–SYK mice compared with controls (mean 506 mg versus 118 mg for control; Figure 1c, Supplementary Figure S1). Spleen weights of ITK–SYK mice were twofold increased (mean 255 versus 121 mg for control; Figure 1c), whereas spleens of SYK wt mice were normal up to 200 days after transplantation. Western blot analysis of spleens or BM of diseased mice showed expression of the respective oncogene (Supplementary Figure S2). Liver weights were normal for all transplantation groups (Supplementary Figure S3).

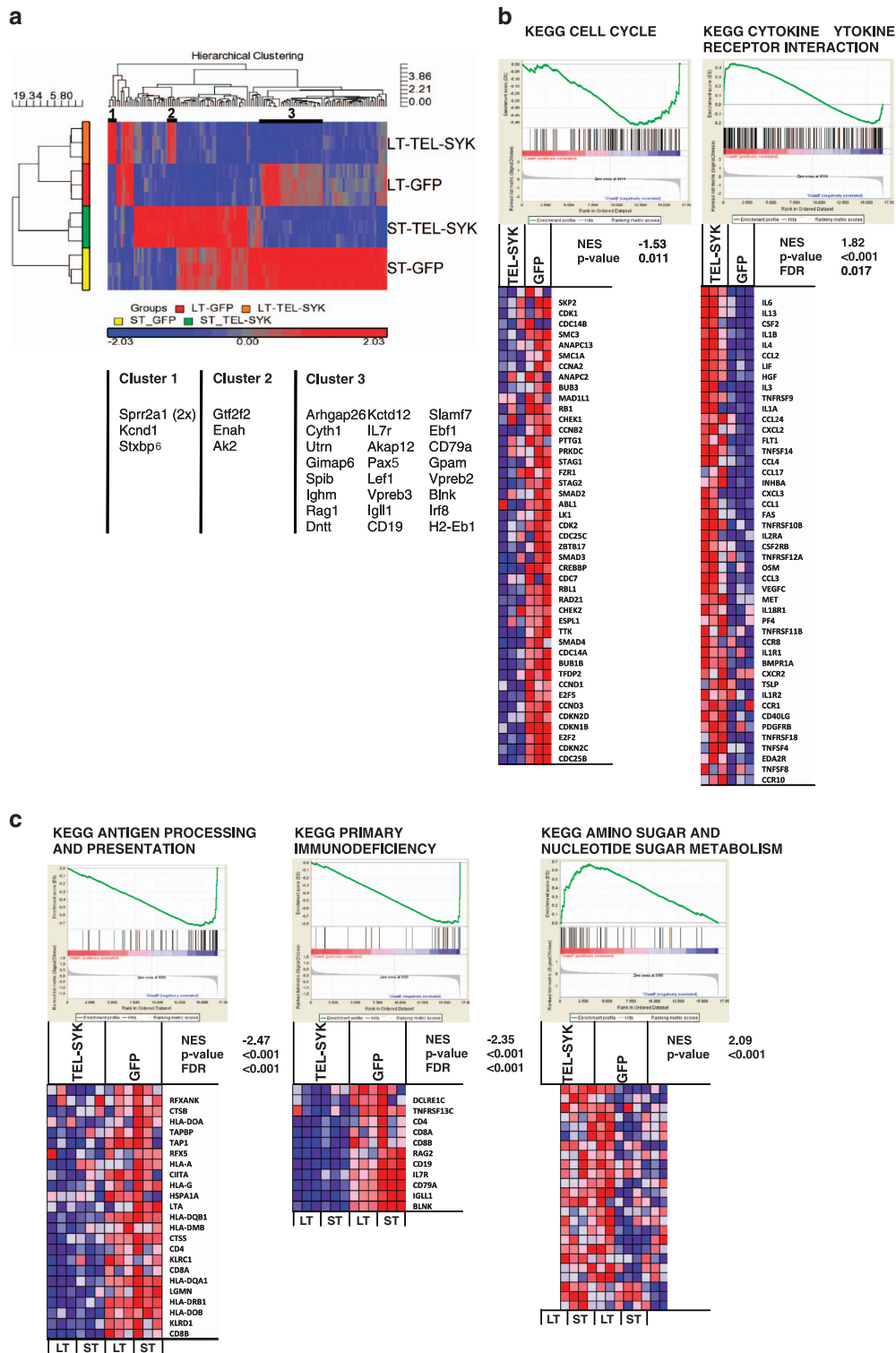Blood analysis of SYK^wt mice showed no lasting alterations in red blood cell counts, white blood cell (WBC) counts,

a

Cluster 1

Sprr2a1 (2x)
Kcnd1
Stxbp6

Cluster 2

Gtf2f2
Enah
Ak2

Cluster 3

Arhgap26	Kctd12	Slamf7
Cyth1	IL7r	Ebf1
Utrn	Akap12	CD79a
Gimap6	Pax5	Gpam
Spib	Lef1	Vpreb2
Ighm	Vpreb3	Blnk
Rag1	Igll1	Irf8
Dntt	CD19	H2-Eb1

b

c

Figure 4. Hierarchical clustering and Gene set enrichment analysis (GSEA) of differentially expressed genes in TEL–SYK or GFP LKS subpopulations. (**a**) Hierarchical clustering was used to visualize genes that were differentially expressed between the four analyzed subpopulations compared to the median expression levels among the groups with a false discovery rate (FDR) < 0.005. Blue shades indicate a lower gene expression level than the median, whereas red shades indicate higher gene expression levels. Three clusters can be identified which are specific for TEL–SYK-expressing LT-HSCs and/or ST-HSCs. The gene names are listed for each cluster. (**b**) Enrichment plots and heat maps for core enrichment genes were generated by GSEA using the KEGG gene sets. NES, nominal *P*-value and FDR are shown for each gene set. Complete gene set lists are available in Supplementary Table 4. Comparison of TEL–SYK versus GFP ST-HSCs identifies downregulation of the 'Cell Cycle' gene set and upregulation of the 'Cytokine Cytokine Receptor Interaction' gene set. (**c**) Comparison of TEL–SYK versus GFP ST- and LT-HSCs identifies downregulation of the 'Antigen Processing and Presentation' and 'Primary Immunodeficiency' gene sets and upregulation of the 'Amino Sugar and Nucleotide Sugar Metabolism' gene set.

thrombocytes or GFP content over a time period of 200 days (Figure 1d, Supplementary Figure S4). In contrast, TEL–SYK mice developed an anemia with a decrease of the red blood cell count to half of that observed in the control group (TEL–SYK mean 4.4×10^6 cells/µl versus control 9.3×10^6 cells/µl) and a reduced hematocrit of 29.4% (control 45.0%; Figure 1d). Also thrombocytes
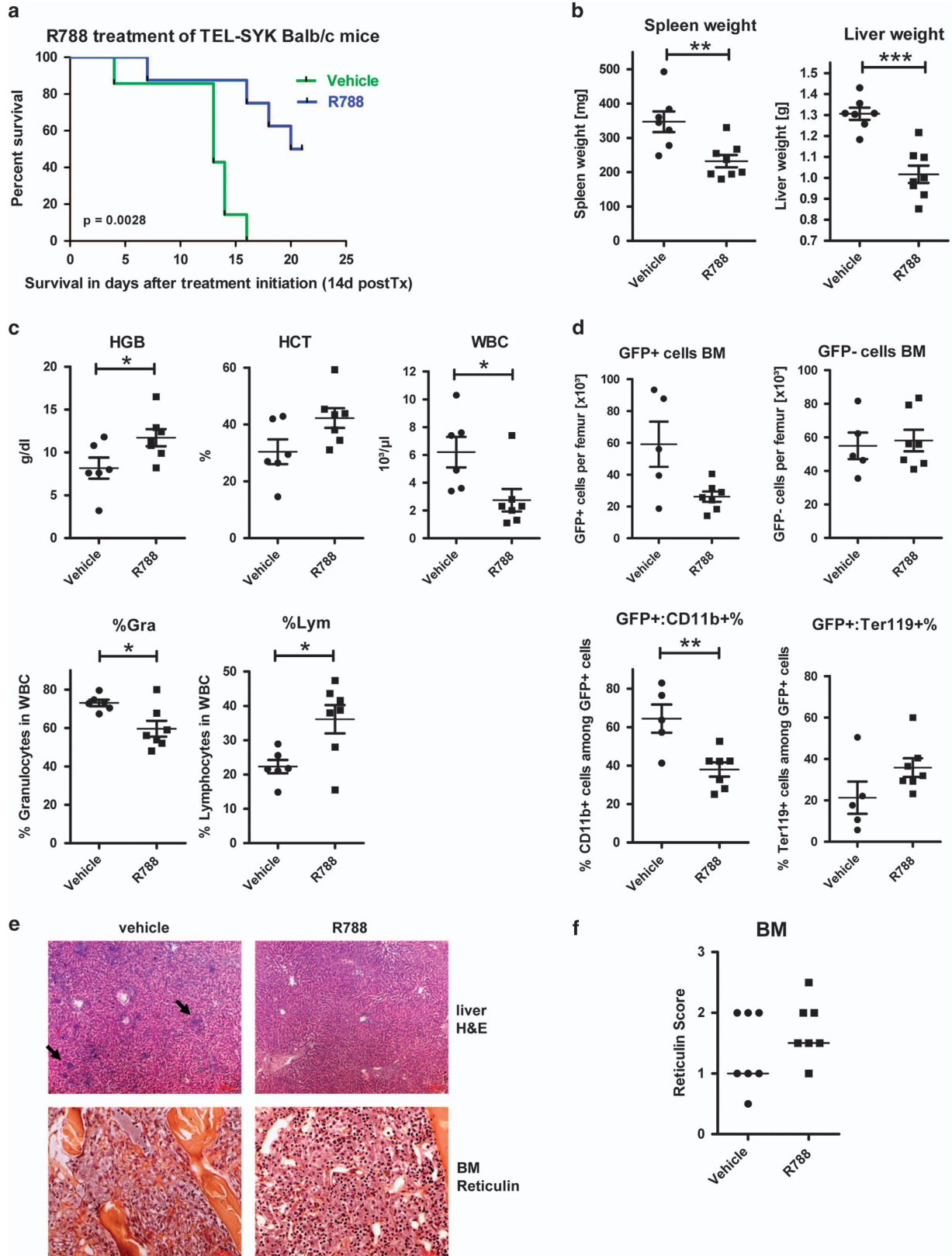
were strongly reduced (TEL–SYK mean 45.7×10^3 cells/µl versus control 583.3×10^3 cells/µl). Furthermore, TEL–SYK mice developed a leukocytosis with a 10-fold increase in WBCs compared with controls (TEL–SYK mean 35.0×10^3 cells/µl versus control 3.1×10^3 cells/µl; Figure 2a). Blood smears stained with May-Grünwald/Giemsa showed accumulation of mature granulocytes in the peripheral blood (Figures 1e and f), but also the occurrence of 9–15% immature blasts as signs of a leukemic disease (Figure 1f and Supplementary Table 1). Flow cytometry analysis revealed that the GFP+ population in TEL–SYK mice mainly consisted of CD11b+/Gr-1+-positive myeloid cells (TEL–SYK 85.56% versus control 38.9%), whereas CD90+/CD3+ T cells (both CD4 and CD8) and B220+ B cells were suppressed (Figure 1g, Supplementary Table 1, Supplementary Figure S5). The percentage of CD11b+ cells within the GFP-negative population in TEL–SYK mice was only 36.67%, indicating a cell intrinsic effect of TEL–SYK driving the accumulation of myeloid cells in the peripheral blood. Despite the occurance of immature blasts in the blood smears, we could not detect an increase in cKit+ (CD117) immature myeloid cells in the peripheral blood, pointing towards an atypical phenotype of the visualized blasts (Supplementary Figure S5).

In contrast to TEL–SYK, SYK^{wt} and ITK–SYK showed no difference in total leukocytes compared with controls and mice did not develop a myeloproliferative or leukemic disease (Figures 1d and e). Nevertheless, both, SYK^{wt} and ITK–SYK, induced a relative expansion of the myeloid compartment (Figures 1f and g). Hereby, SYK^{wt}, similar to TEL–SYK, induced an expansion of myeloid cells only within the SYK/GFP+ population. In contrast, ITK–SYK enhanced myeloid cells and reduced B220+ cells within the GFP+ and GFP– population, pointing towards a cell extrinsic effect as driver for myeloid expansion and B-cell suppression in those mice (Figure 1g).

SYK oncogenes drive myeloid and T-cell expansion and alter the HSC pool

To further characterize the disease in TEL–SYK mice, to compare it with the other oncogenes and to discriminate between cell intrinsic and cell extrinsic effects, hematopoietic cell subsets within the GFP+ (oncogene carrying) and GFP– population in spleens and BM were analyzed by flow cytometry. Transplantation groups were compared at 25 days (final disease for TEL–SYK) and 42 days (final disease for ITK–SYK) after transplantation.

Interestingly and consistent with the findings from the peripheral blood, the GFP+ cells in the BM and spleens of TEL–SYK mice consisted of more than 90% myeloid cells (CD11b+), whereas B cells (B220+), erythroid progenitors (Ter119+; BM) and T cells (CD3+/CD90+; spleen) were suppressed (Figure 2a, Supplementary Table 2). Furthermore, we detected a significant decrease in Lin-cKit+ myeloid progenitors in the BM and also a

reduction of Lin-Sca1+ lymphoid progenitors within the GFP+ population (Figure 2b). Relative amounts of LKS cells (percentage of Lin-cKit+Sca+ cells within complete BM) in the BM and spleens were also strongly reduced (Figures 2b and c). Further analysis of LKS subpopulations showed a dramatic reduction of total LT-HSCs and ST-HSCs and to a lower extent also of the MPP population in TEL–SYK mice (Figure 2d). Cell cycle analysis of TEL–SYK+ LKS cells by DNA staining showed reduced cells in S/G2 phase compared with controls (Figure 2e). Further analysis of the cell cycle status of all LKS subpopulations (LT/ST/MPP cells) and myeloid progenitors in the BM was performed by EdU in vivo staining for 15 h and confirmed the reduction of cycling cells mainly within the LT and ST-HSC compartment (Figure 2f).

In concordance with the loss of nearly all stem- and progenitor populations in BM and spleens, total cell counts in femurs and spleens of TEL–SYK mice were strongly reduced compared with control mice (femur control 7.3×10^6 total cells versus femur TEL–SYK 0.75×10^6 total cells), resulting in a dramatic loss of all cell types including myeloid cells and all progenitor subtypes in both organs (Figure 2g).

Retransplantation of 2 million cells isolated from the BM of TEL–SYK mice into secondary recipient mice did not induce engraftment of the disease, pointing towards the MDS phenotype as a major event caused by the fusion.

In contrast to TEL–SYK, total cell numbers in femurs and spleens of ITK–SYK mice were equal (or slightly increased in spleen) compared with GFP controls (Figure 2d). Analysis of the GFP+ population of ITK–SYK mice revealed a significant increase in myeloid cells in BM and spleens, although this increase within the GFP+ population was much lower than seen in TEL–SYK mice (Figure 2a). In concordance with results from the peripheral blood, the GFP– population also showed an increase in myeloid BMCs as sign of a cell extrinsic effect driving the myeloid expansion. Although B cells and erythroid cells (Ter119) were suppressed, we detected a significant increase of CD4+ and CD8+ T cells within the GFP+ population in the BM reflecting the previously described T-cell lymphoproliferative/lymphoma disease induced by ITK–SYK (Figure 2a, Supplementary Figure S6, Supplementary Table 2). Interestingly, and in contrast to TEL–SYK, ITK–SYK also strongly enhanced the Lin-Kit-Sca+ population (Figures 2b and c) and the Kit-Sca+B220+ lymphoid progenitor (CLPII) compartment within the GFP+ population (Supplementary Table 1) and induced a 10-fold expansion of LKS cells in BM and spleens within only 45 days (Figures 2b and c; Supplementary Table 2).

SYK^{wt} mice also showed normal total cell numbers in femurs and spleens compared with GFP controls (Figure 2d). Relative cell distribution showed features of both, the TEL–SYK and ITK–SYK phenotype, with a cell intrinsic expansion of the myeloid compartment in the BM and the T-cell compartment in the spleen (Figure 2a). B cells and Ter119+ erythroid progenitors were reduced (Figures 2a–d; Supplementary Table 2).

Figure 5. SYK inhibitor treatment prolongs survival of TEL–SYK mice, but cannot reduce myelofibrosis. (a) Kaplan–Meier survival curve of R788 treated ($n = 8$) versus vehicle-treated ($n = 7$) Balb/c mice transplanted with the TEL–SYK oncogene. Treatment started 2 weeks after transplantation. Vehicle mice died within 16 days after treatment initiation, whereas R788 treated mice were killed after 21 days, when significance was reached (log-rank test) and to compare organ infiltration. (b) Spleen and liver weights of both treatment groups compared at the survival end point. R788 treated mice had a 1.5-fold decrease in spleen weight and 1.3-fold decrease in liver weight. *$P < 0.05$; **$P < 0.01$; ***$P < 0.001$, unpaired t-test. (c) Peripheral blood analysis of R788 treated ($n = 7$) versus vehicle-treated ($n = 6$) Balb/c mice 14 days after treatment initiation using hemoglobine (HGB), hematocrit (HCT), WBC and percentages of granulocytes and lymphocytes. *$P < 0.05$; **$P < 0.01$; ***$P < 0.001$, unpaired t-test and Mann–Whitney test for WBC. (d) Flow cytometry analysis of GFP+ and GFP– cells in the BM as well as GFP+/ CD11b+ and GFP+/ Ter119+ BM cells 16 days (vehicle treated) and 21 days (R788 treated) after treatment initiation. *$P < 0.05$; **$P < 0.01$; ***$P < 0.001$, unpaired t-test. (e) Hematoxylin and eosin-stained liver slides and reticulin stained BM slides are shown from one R788 treated mouse versus control mouse. Arrows show liver infiltrates in the control group, which are absent in the treatment group. (f) Grading of fibrosis in BM slides for vehicle treated versus R788 treated Balb/c mice ($n = 7$). Grade 1 shows a slight expansion of reticulin fibers, grade 2 represents a dense network of reticulin fibers, whereas grade 3 shows a strong expansion of collagen fibers with osteoneogenesis. Grading was done by two researchers blinded to the group attribution by considering reticulin staining in three fields of vision at × 100 magnification.
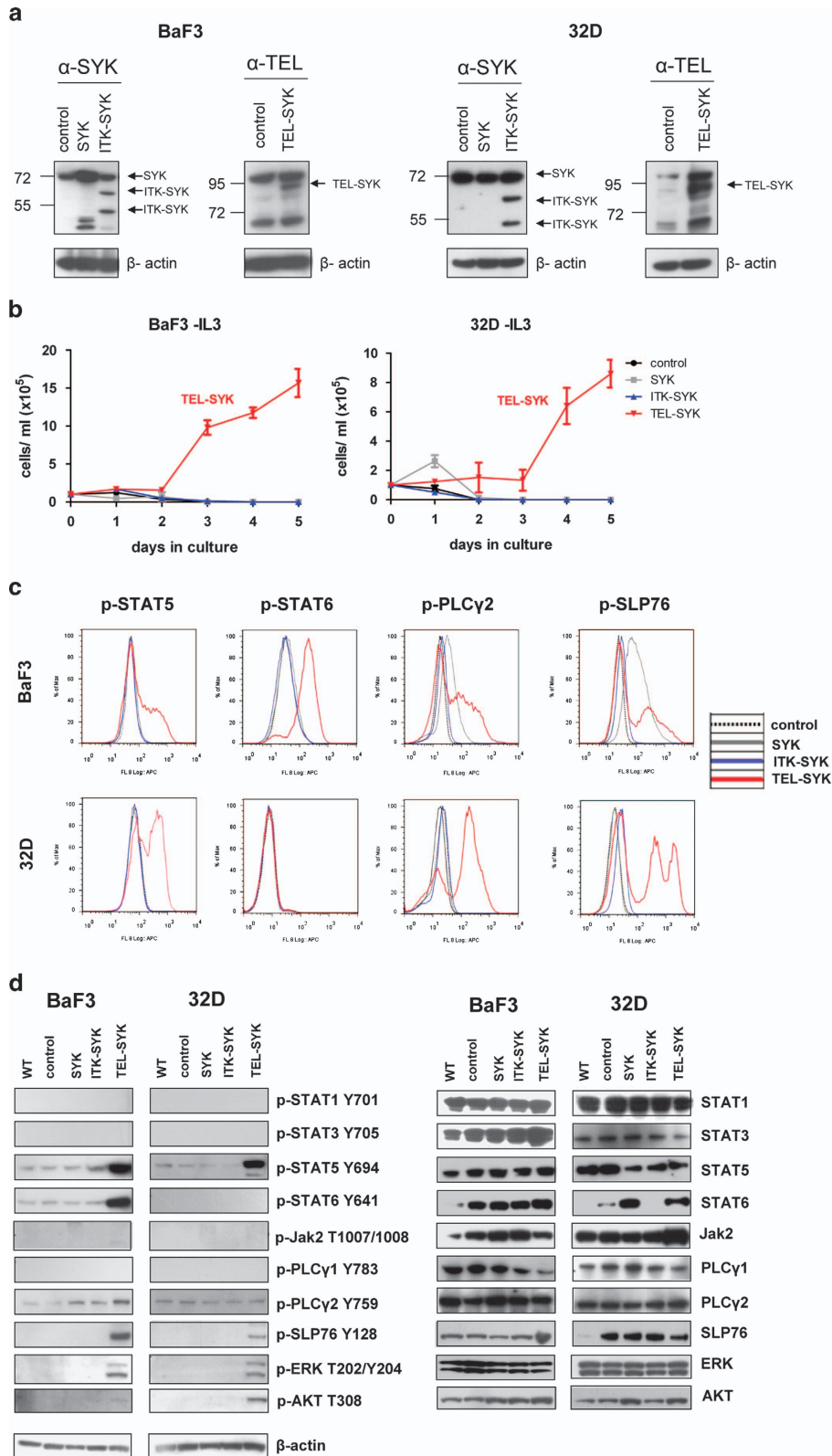
Figure 6. TEL–SYK exclusively induces factor independency and STAT5/6 phosphorylation in myeloid and B-lymphoid cells. (**a**) Expression of SYK^wt, ITK–SYK and TEL–SYK after retroviral infection and GFP-sorting of the IL-3 dependent cell lines BaF3 and 32D. For detection of SYK^wt and ITK–SYK by western blot, a primary SYK antibody was used. For detection of TEL–SYK, we used a TEL antibody. (**b**) Growth curves for IL-3-depleted BaF3 and 32D cells expressing the different oncogenes over 5 days were performed by counting Trypan blue negative cells via Neubauer chamber. (**c**) Intracellular phospho flow cytometry for phosphorylated STAT5/6, PLCγ2 and SLP76 in BaF3 cells (upper panel) and 32D cells (lower panel) expressing the different constructs. (**d**) Western blot of BaF3 and 32D cells expressing either control vector or the different SYK oncogenes with antibodies against phosphorylated STATs, PLCγ, JAK2, SLP76, ERK and AKT. Left panel shows the phosphorylated protein, right panel the total protein.

TEL–SYK induces an AML with features of human acute panmyelosis with myelofibrosis in mice

To further characterize the disease in TEL–SYK mice, hematoxylin and eosin stainings, periodic acid–Schiff staining and reticulin staining were performed from BM, spleens and livers of the diseased mice and all slides were examined by a mouse pathologist.

BM from TEL–SYK mice showed signs of multilineage dysplasia as seen in myelodysplastic syndrome, with hypoplasia of erythrocytes showing nuclear fragmentation, irregular nuclear contours and abnormal mitotic figures. Myelopoesis showed abnormal nuclear maturation with open chromatin, lobulated nuclei and hypogranulation. Immature megakaryocytes/megakaryoblasts were strongly increased reaching up to 50% of total cell counts and partially displayed multiple separated nuclei or unlobulated nuclei as well as micromegakaryocytes (Figure 3a, Supplementary Figure S7). Megakaryocytes were mainly periodic acid–Schiff stain positive (Figure 2b) and were organized in clusters. The immature megakaryoblasts in the BM were phenotypically identical with blasts seen in the peripheral blood. Reticulin staining showed a grade 2–3 myelofibrosis, at least partially explaining the reduced total cell counts in TEL–SYK mice (Figure 3c, Supplementary Figure S7). TEL–SYK spleens had lost their normal follicular architecture, were strongly fibrotic and were infiltrated with myeloid cells, predominantly consisting of mature granulocytes, dysplastic erythrocytes and clusters of dysplastic and immature megakaryocytes (Figure 3c). The same cell types also infiltrated the liver (Figure 3a). Taken together and according to the Bethesda classification of nonlymphoid hematopoietic neoplasms in mice[44] (myeloid disorders), the TEL–SYK phenotype in the majority of mice can be classified as AML with features of human acute panmyelosis with myelofibrosis (APMF). Due to the frequent MDS features, we also have to consider the diagnosis of a myelodysplastic syndrome with features of human refractory anemia with excess blasts and fibrosis (RAEB-F) and at least one mouse, with more than 50% megakaryoblasts in the BM can be diagnosed as megakaryocytic leukemia.

In contrast to TEL–SYK, ITK–SYK mice showed neither signs of dysplasia nor myelofibrosis in the BM nor displayed any accumulation of immature megakaryocytes (Figures 3a–c). Overlapping with TEL–SYK mice, granulopoiesis was enhanced in BM and spleens and even infiltrated the liver. Additionally and consistent with our previous publication, we also found infiltration of T cells into the spleenic lymph follicles, the BM and the liver, reflecting the previously described lymphoproliferative disease caused by ITK–SYK.[33]

SYK[wt] mice had a normal splenic and BM architecture and no liver infiltration (Supplementary Figure S7). Compared with GFP controls and consistent with our flow cytometry data, SYK[wt] mice had enhanced relative numbers of mature granulocytes in BM and spleens.

TEL–SYK alters the gene expression profile of LKS subpopulations and downregulates genes important for B-cell development and cell cycle regulation

To further characterize the effect of TEL–SYK on the stem cell compartment, we sorted TEL–SYK+ LT-HSCs (Lin-Kit+Sca+CD150+FLT3-) and ST-HSCs (Lin-Kit+Sca+CD150-FLT3-) and compared them with control counterparts by gene expression profiling. Hundred and eight genes with a P-value < 0.005 discriminated between the different groups and are shown by gene cluster analysis (Figure 4a and Supplementary Table 3). Gene cluster 1 shows genes exclusively overexpressed in TEL–SYK LT-HSCs. Gene cluster 2 shows genes overexpressed in TEL–SYK LT and ST-HSCs compared with GFP controls and cluster 3 shows genes downregulated in TEL–SYK+ LT and ST-HSCs. Genes identified in cluster 1 and elevated in TEL–SYK LT-HSCs are Sprr2a1 (2x), Kcnd1

(potassium voltage gated channel) and Stxbp6 (syntaxin binding protein 6). In cluster 2, we found Gtf2f2 (general transcription factor 2 F), Enah (Mena, associated with epithelial-mesenchymal transition in solid tumors) and Ak2. Ak2 was described as being mutated in reticular dysgenesis leading to loss of neutrophils and lymphocytes[45] and might therefore be involved in the MPN phenotype seen in our mice.

Genes downregulated in TEL–SYK LT and ST-HSCs (gene cluster 3) are mainly involved in early B-cell development (Blnk, IL7r, Irf8, Rag1 and so on), which fits to our observation that nearly all B cells are lost in TEL–SYK+ mice. Furthermore, we found genes downregulated that are involved in interferon-alpha signaling (Tlrp1,6,7 und 9; Figure 4a).

Gene set enrichment analysis using the KEGG gene set database from TEL–SYK+ versus control ST-HSCs showed downregulation of genes involved in cell cycle regulation (Figure 4b) supporting our in vivo observation of reduced proliferation rates and cell cycle alterations in TEL–SYK+ HSCs. Furthermore, within ST-HSCs, we found the upregulation of the 'cytokine cytokine receptor interactions' gene set with increased levels for IL-6, IL-13, IL-1B, LIF and many others recapitulating the cytokine storm shown in those mice (Figure 4b).[39] Pathways involved in immune regulation, B-cell receptor signaling and antigen processing were reduced, which matches the lymphopenic phenotype of the mice, whereas metabolic pathways were increased (Figure 4c, Supplementary Table 4).

SYK inhibition can partially revert the TEL–SYK-induced phenotype

To investigate if the TEL–SYK-induced APMF leukemia with myelofibrosis and myelodysplasia can be reverted by SYK inhibitor treatment, we treated mice with the R406 prodrug R788 starting 2 weeks after transplantation. SYK inhibitor treatment could significantly enhance the survival of the mice (Figure 5a), reduced the spleen and liver size (Figure 5b) and reduced the WBC count (Figure 5c). Relative lymphocyte counts increased, whereas granulocyte counts decreased, bringing relations of both blood components closer to normal state. The hemoglobin levels, the hematocrit and total erythrocyte counts after 14 days of treatment were significantly enhanced (Figure 5c). Comparison of cell subsets in the BM reflected the results from the peripheral blood with reduced neutrophils (CD11b+ cells) and enhanced Ter119+ erythroid progenitors in GFP+ and GFP – populations (Figure 5d). The GFP+ population in the BM was strongly reduced after treatment with R788, whereas total GFP – cells were not affected (Figure 5d). IHC staining also showed repopulation of the BM with erythroid progenitors and a reduction of megakaryoblast infiltration (Figure 5e). Liver infiltration by granulocytes and megakaryoblasts was nearly absent in the R788 treatment group (Figure 5e).

Interestingly, and in contrast to our expectations, myelofibrosis was not significantly reduced in the treatment group according to our reticulin staining (Figure 5f), which might indicate that this process once initiated, is not reversible by SYK inhibition in late stages of the disease.

TEL–SYK exclusively induces IL-3 independent growth and STAT5/6 phosphorylation in myeloid and B-lymphoid cells

To further examine the differences in signal transduction between TEL–SYK, SYK[wt] and ITK-SYK dependent on the background of the transformed cell, we overexpressed the oncogenes in myeloid (32D cells) and B-lymphoid (BaF3 cells) cell lines (Figure 6a).

Interestingly, only the overexpression of TEL–SYK, but not ITK–SYK or SYK[wt], induced growth factor independence of the otherwise IL-3-dependent 32D- and BaF3 cells (Figure 6b). Therefore, we aimed to identify signaling pathways specifically activated by TEL–SYK and performed western blots with phospho-specific antibodies and additionally phospho-flow cytometry (Figures 6c and d,

12

Supplementary Figure S8). Myeloid 32D cells carrying TEL–SYK showed an exclusive activation of STAT5, SLP76 and PLCγ2 (p-PLCγ2 by flow cytometry), ERK and AKT. In B-lymphoid BaF3 TEL–SYK cells, we found a similar activation pattern with phosphorylation of STAT5, SLP76, PLCγ2 and ERK, no AKT phosphorylation, but additionally activation of STAT6.

In contrast, SYK^{wt} and ITK–SYK did not activate any of those pathways in 32D cells (Figures 6c and d), but SYK^{wt} was able to
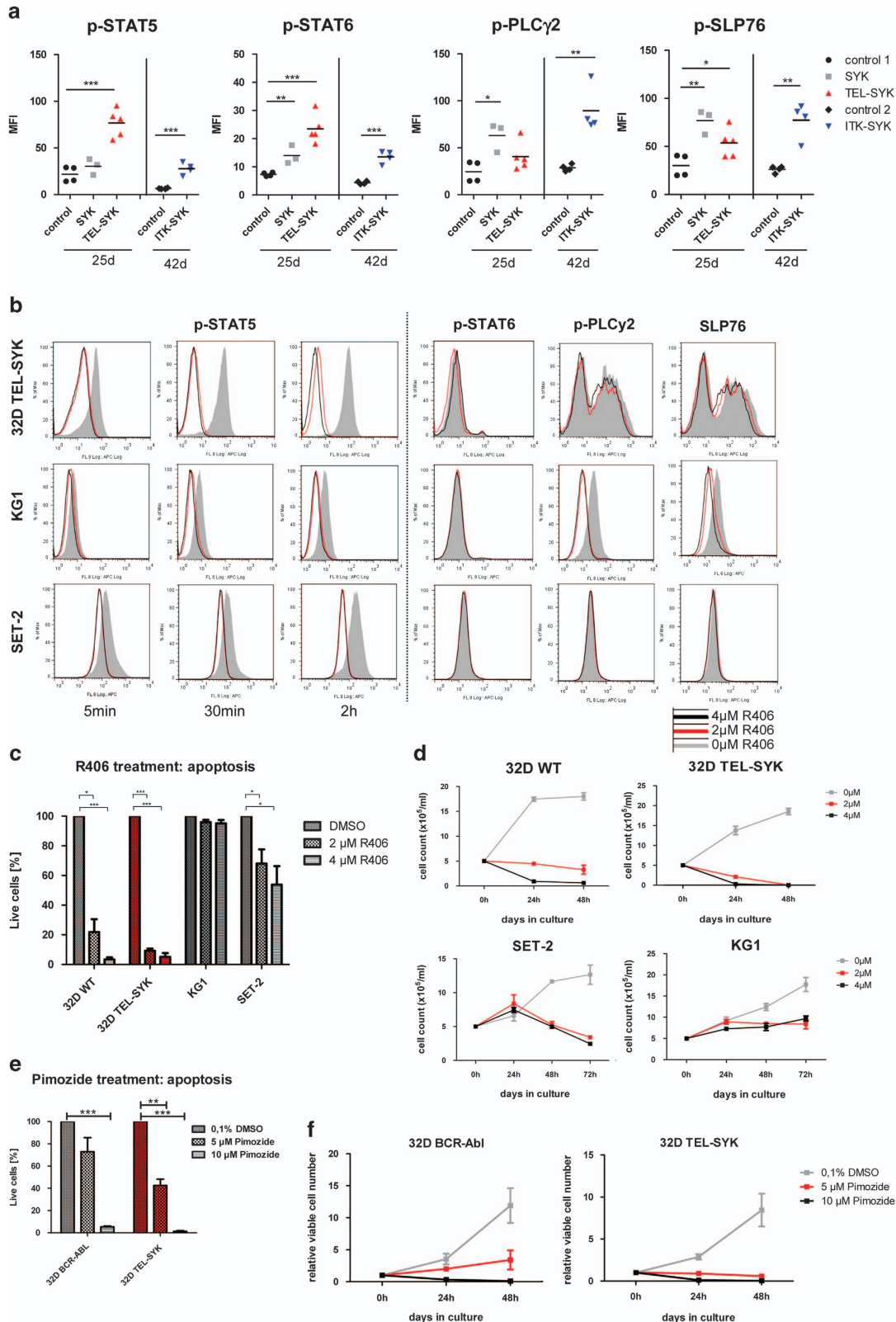
activate PLCγ2 and SLP76 in BaF3 cells as assessed by flow cytometry (Figure 6c).

STAT5 is an essential downstream target of TEL–SYK in vivo and is generally regulatable by SYK inhibitors

To verify if any of those pathways activated by the SYK oncogenes in vitro is also relevant in vivo, we analyzed BM and spleen cells of SYK oncogene carrying mice by using phospho-flow cytometry of GFP+ cells. TEL–SYK positive murine myeloid cells showed a strongly increased phosphorylation of STAT5 and STAT6 in vivo, supporting the in vitro results (Figure 7a). In contrast, other phosphorylation events like PLCγ2 activation could not be confirmed in vivo and SLP76 phosphorylation was only moderately increased. The phosphorylation pattern of SYK^wt cells was completely different, with a strongly increased phosphorylation of PLCγ2 and SLP76, but not STAT5 and STAT6, which is in line with the in vitro results. According to those findings, we hypothesized that STAT5 and STAT6 phosphorylation, but not SLP76 and PLCγ2, make the difference in between malignant transformation caused by TEL–SYK or only myeloid expansion as caused by SYK^wt. STAT5 is known to be a major player in oncogenic transformation of myeloid cells and is activated in myeloproliferative diseases and different types of AML. To verify that STAT5 is directly regulated by the oncogenic TEL–SYK kinase fusion in myeloid cells, we treated TEL–SYK 32D cells with the SYK inhibitor R406 for up to 2 h. SYK inhibition in TEL–SYK 32D cells resulted in a fast dephosphorylation of STAT5 within 10 min and induction of apoptosis and reduced proliferation in the absence of IL-3 (Figures 7b–d). SYK inhibition did not reduce STAT6 phosphorylation nor phosphorylation of SLP76 or PLCγ2 within these 2 h, pointing towards those genes as secondary phosphorylation events.

Previously published results point toward SYK as a major driver of human AML and SYK inhibition or depletion resulted in differentiation and reduced proliferation of AML cell lines.[31] In concordance with those previous reports, SYK inhibition in the human AML cell line KG-1 reduced proliferation of those cells while not inducing apoptosis (Figures 7c and d). Furthermore, SYK inhibition resulted in the dephosphorylation of STAT5, but also PLCγ2 and SLP76. As the murine TEL–SYK model reflects features from a classical AML, but also characteristics of a megakaryocytic leukemia with accumulation of megakaryoblasts in the BM and myelofibrosis, we chose the human cell line SET-2 for further experiments. SET-2 cells were obtained from a patient with secondary megakaryocytic leukemia evolving after a long period of diagnosis with essential thrombocytosis (ET) and positive for JAK2V617F. Treatment of SET-2 cells with R406 resulted in an exclusive reduction of STAT5 phosphorylation, as well as induction of apoptosis and reduced proliferation.

Taken together, SYK inhibition in different cell lines seems to merge in STAT5 dephosphorylation and can affect proliferation and viability of AML cells and megakaryocytic leukemia cells, despite their dependence on other oncogenes.

To further validate the role of STAT5 in TEL–SYK-induced transformation, 32D TEL–SYK cells were treated with the STAT5 inhibitor Pimozide. Pimozide treatment resulted in significant apoptosis induction and reduced proliferation, similar to that seen with the SYK inhibitor R406, supporting the role of STAT5 downstream of oncogenic SYK (Figures 7e and f).

Depletion of Stat5 blocks TEL–SYK-induced leukemia and myelofibrosis

To further validate the role of STAT5 downstream of oncogenic SYK, we overexpressed TEL–SYK in BMCs from conditional Stat5^fl/fl Mx1Cre mice versus control Stat5^fl/fl mice.[40] This experimental system was previously used to demonstrate the addiction of BCR–ABL-transformed leukemic cells to Stat5 signaling, whereas normal adult hematopoiesis was rarely affected (mild reduction of hematocrit and thrombocytes within the first 8 weeks of Stat5 depletion).[41] TEL–SYK/Stat5^fl/flMx1Cre BMCs and TEL–SYK/ Stat5^fl/fl control BMCs were transplanted into irradiated recipients and treated with Poly-I:C 7 days after transplantation to allow full engraftment of normal and leukemic cells before depletion of Stat5. Stat5 depletion could be detected by western blot analysis of total Stat5 protein levels and by intracellular phospho-Stat5 staining of hematopoietic cells derived from the BM at the end of the experiment (Figures 8a and b). Thirty-two days after transplantation, the control group developed a lethal disease with leukocytosis and increase in myeloid cells in the peripheral blood and the experiment was terminated. Comparison of the spleens showed a dramatic difference with TEL–SYK control spleens being enlarged to a medium weight of 630 ± 79 mg, whereas TEL–SYK/Stat5 − / − spleens were normal in size and weight (mean 121 ± 9 mg; Figures 8c and d). Analysis of the peripheral blood at the time of death revealed a leukocytosis in the TEL–SYK control group with an average of 40×10^3 cells/μl mainly consisting of mature granulocytes, whereas TEL–SYK/ Stat5 − / − mice had normal WBC counts in between 1 and 3×10^3 cells/μl (Figures 8e and f) without enhancement of the myeloid population. Further analysis of BMCs and spleen cells showed, that the Stat5 − / − did not only prevent the expansion of TEL–SYK+ myeloid cells, but blocked the expansion of the complete TEL–SYK + population (GFP+ cells within total BMCs; Figure 8f). Histological evaluation revealed that not only the AML phenotype (liver and spleen infiltration with immature blasts, leukocytosis) was suppressed by the depletion of Stat5, but that also myelofibrosis was abrogated (Figure 8h), pointing toward Stat5 as the major mediator of TEL–SYK-induced disease development.

Figure 7. TEL–SYK induces activation of STAT5 in vivo. (a) Intracellular phospho flow cytometry for p-STAT5/6, p-PLCγ2 and p-SLP76 of GFP+ myeloid spleen cells coming from control, SYK^wt, ITK–SYK and TEL–SYK-transplanted Balb/c mice. Graphs show the mean fluorescence intensity (MFI) per mouse. TEL–SYK shows highest activation of STAT5 and STAT6 in vivo, whereas SYK and ITK–SYK show a strong activation of PLCγ2 and SLP76. *$P < 0.05$; **$P < 0.01$; ***$P < 0.001$, unpaired t-test. (b) Intracellular phospho-flow cytometry for phosphorylated STAT5/6, PLCγ2 and SLP76 of 32D TEL–SYK cells, KG-1 cells (AML cell line) and SET-2 cells (megakaryocytic leukemia cell line) treated with the SYK inhibitor R406 for 5 min, 30 min or 2 h. For p-STAT6, p-PLCγ2 and p-SLP76 only the 30 min time point is shown. (c) 32D cells with IL-3, 32D TEL–SYK cells without IL-3, KG-1 cells and SET-2 cells were all treated with R406 for 48 h and apoptosis was assessed by AnnexinV/7-AAD staining. Graph shows the mean relative percentage of viable cells (AnnexinV-/7-AAD-) compared with the dimethylsulfoxide (DMSO) control +s.e.m from three independent experiments ($n = 3$). (d) Total viable cell numbers were assessed by counting the cells with a Neubauer counting chamber after treatment with SYK inhibitor over 48–72 h. Graphs are shown for the DMSO control, the 2 μM and the 4 μM R406 concentration for 32D cells+IL-3, 32D TEL–SYK cells without IL-3, KG-1 cells and SET-2 cells. (e) 32D BCR–ABL and 32D TEL–SYK cells grown without IL-3 were treated with 5 and 10 μM pimozide for 48 h and apoptosis was assessed by AnnexinV/7-AAD staining. Graph shows the mean relative percentage of viable cells (AnnexinV-/7-AAD-) compared with the DMSO control+s.e.m from three independent experiments ($n = 3$). *$P < 0.05$; **$P < 0.01$; ***$P < 0.001$, paired t-test. (f) Growth curves of 32D BCR–ABL and 32D TEL–SYK cells grown without IL-3 and treated with DMSO, 5 and 10 μM pimozide were performed over 48 h in three independent experiments ($n = 3$) by counting Trypan blue negative cells in a Neubauer chamber.
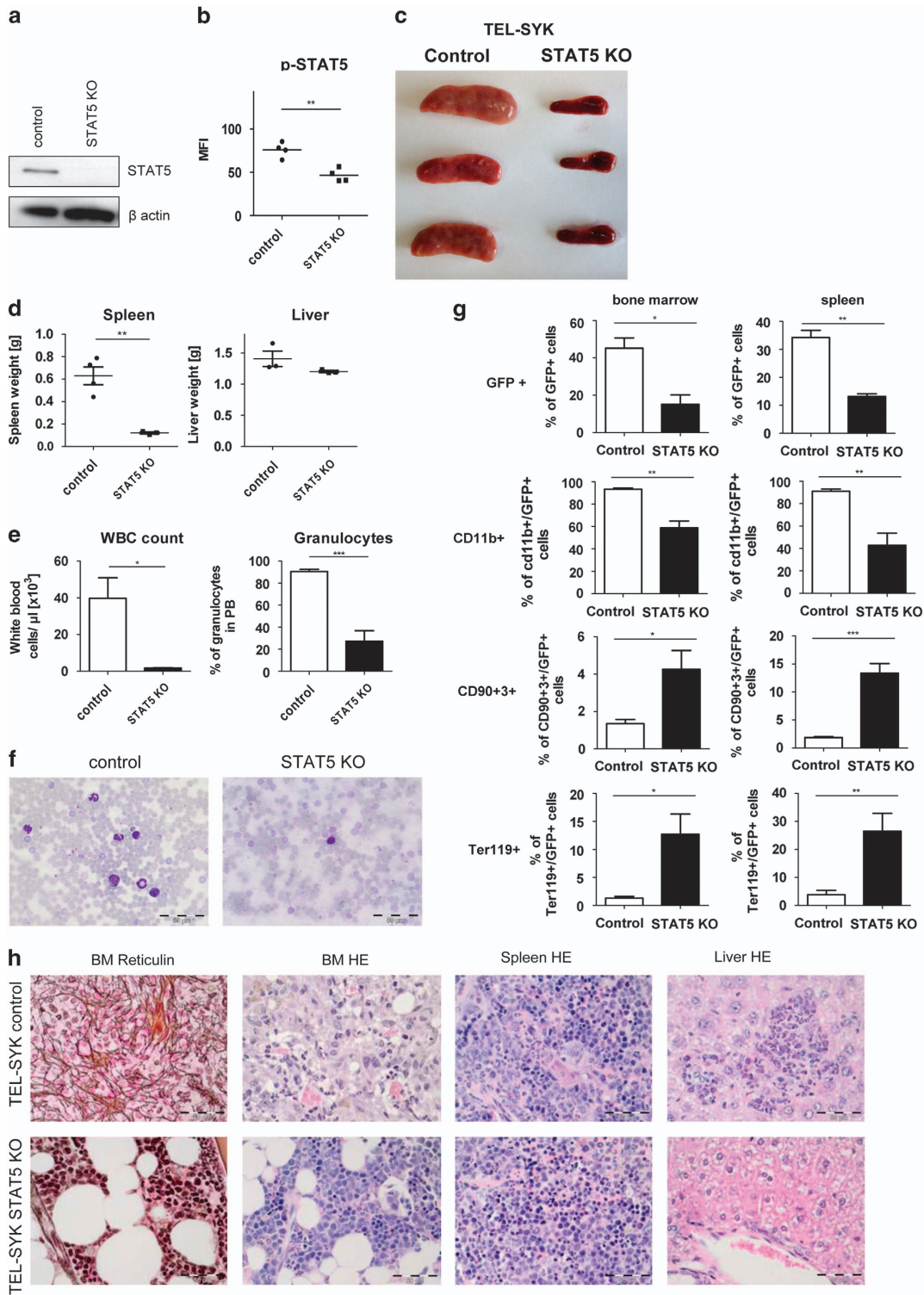

Figure 8. Depletion of Stat5 blocks TEL–SYK-induced leukemia and myelofibrosis. (**a**) Western blot showing depletion of Stat5 in $Stat5^{fl/fl}Mx1Cre$ BMCs versus control $Stat5^{fl/fl}$ BMCs from mice treated with three times injection of Poly (I:C) and 35 days after transplantation. (**b**) Intracellular phospho-Stat5 staining was assessed by flow cytometry from BMCs from mice treated as in A ($n = 4$ per group). (**c**) Photograps showing spleens of three TEL–SYK control and three TEL–SYK Stat5$^{-/-}$ mice in comparison after 35 days. (**d**) Spleen and liver weights from TEL–SYK control and TEL–SYK Stat5$^{-/-}$ mice. (**e**) Peripheral blood of TEL–SYK control and TEL–SYK Stat5$^{-/-}$ mice ($n = 4$) was analyzed for red blood cell count, hematocrit, WBC count, thrombocytes and granulocytes 35 days post transplantation with the ADVIA120 blood analyzer. Graphs show results for total WBCs and the percentage of granulocytes. (**f**) Photographs from blood smears of control TEL–SYK and TEL–SYK Stat5$^{-/-}$ mice, which were stained with May-Grünwald/Giemsa. Bars, 50 μm. (**g**) GFP contents, CD11b+/GFP+ expression, CD90+3+/GFP+ expression and Ter119+/GFP+ expression within total live cells was assessed by flow cytometry analysis in BM and spleen cells from TEL–SYK control and TEL–SYK Stat5$^{-/-}$ mice 35 days after transplantation ($n = 4$). *$P < 0.05$; **$P < 0.01$; ***$P < 0.001$, unpaired t-test. (**h**) Representative images showing hematoxylin/eosin and reticulin (left image) stained BM, spleen and liver slides from TEL–SYK control and TEL–SYK Stat5$^{-/-}$ mice. Bars, 50 μm.

DISCUSSION

Oncogenic SYK was found to be an important driver of different hematologic malignancies.[26,27,29,46] In our study comparing the different SYK oncogenes in mice, we could confirm the diverse picture of SYK involvement in human disease, with ITK–SYK driving T-cell neoplasias[32] and TEL–SYK inducing an AML phenotype. Interestingly, myeloid expansion was seen with all SYK oncogenes, even with SYK[wt], pointing toward this cell type as being most susceptible to alterations in expression and activation levels of the SYK kinase. Interestingly, myeloid expansion was not always driven by a cell intrinsic effect as seen with the TEL–SYK oncogene, but was partially driven by cell extrinsic effects at least in the ITK–SYK mouse model. ITK–SYK caused a cell intrinsic T-cell expansion in the BM, which induced a strong cell extrinsic (GFP+ and GFP − cells) expansion of the myeloid compartment and even a 10-fold increase in the LKS compartment. Several cytokines, like interferon-γ and IL-5, were reported to be highly upregulated in the ITK–SYK mouse model[33] and might cause this phenomenon.

Interestingly, SYK[wt]-expressing mice showed an intermediate phenotype with a cell intrinsic myeloid, but also T-lymphoid expansion. In contrast to the other two oncogenes, SYK[wt] is not bound to a certain cell compartment, but can still alter its localization and despite its overexpression is still controllable by cell intrinsic regulatory processes like phosphorylation events or protein degradation. In contrast, TEL–SYK is constitutively activated by the TEL oligomerization domain and is fixed in the cytoplasm, which might be causative for the exclusive myeloid, but not T-lymphoid expansion. Despite our expectations, we could not detect an expansion of the B-cell population, although SYK[wt] is thought to be a target in a broad spectrum of B-cell lymphoma subtypes.[26,27,29,46] This might on one hand argue for a minor role of SYK in B-cell malignancies, but could also be caused by our experimental design of using 5-Fluorouracil-pretreated BM, which has lost most of the target B cells for the retroviral infections.

The TEL–SYK phenotype seen in the mice strongly resembles the disease from the patient, where the fusion kinase was originally identified.[35] Both mice and men show an MDS phenotype in the BM with signs of dysplasia in the erythroid and megakaryocytic lineage. In both cases, there was a myeloid hyperplasia and an increase in immature blasts with a megakaryocytic phenotype in the BM. The patient later progressed to AML with megakaryocytic blasts. According to the new WHO classification of 2008 and the Bethesda classification for murine leukemias, the disease can be characterized as AML with features of human APMF. The fact that the disease is not retransplantable does not interfere with this diagnosis, as the other main criteria for AML (more than 20% blasts in the BM and lethal disease within 4 weeks) are fulfilled. A recently published paper, where the investigators overexpressed TEL–SYK in fetal liver cells, shows part of the phenotype that we observe in our mice.[39] The authors describe the same MDS and MPN features (granulocytosis, myelofibrosis), but the disease is not in all cases lethal and mice succumb to disease at a much later time point at 60 days after transplantation. Furthermore, the mice do not accumulate megakaryoblasts in the BM (as described here and in the patient) and also have no blasts in the peripheral blood and can therefore not be diagnosed as leukemia. The major difference in our experimental procedures is the use of adult BM instead of fetal liver cells. To further support our diagnosis, we overexpressed the TEL–SYK oncogene not only in Balb/c mice, but also C57BL/6 mice, and also here, we find the APMF phenotype with infiltration of the BM and liver with megakaryoblasts (data not shown).

One mouse with more than 50% megakaryocytic blasts in the BM has even reached the criteria for a megakaryocytic leukemia bringing megakaryocytic disorders into the focus of our research. SYK is highly expressed within the megakaryocytic lineage[47] and was previously shown to be essential for migration of megakaryocytes from the BM niche towards the vascular niche.[48] In megakaryocytes and other hematopoietic cells, the SYK kinase has a critical role in the inside-out activation of integrins by glycoprotein receptors such as the collagen receptor GPVI.[49–51] In addition, SYK has an important role in outside-in signals from integrins that mediate changes in cytoskeletal organization leading to cell spreading and motility.[52] Megakaryocytic maturation is guided by microenvironmental factors provided by different niche cell subsets and platelet release only occurs in the vascular niche. Therefore, alterations in migration as induced by alterations in SYK activity[48] could strongly affect the maturation processes and also the functionality of megakaryocytes and argues for a tight regulation of SYK expression as necessary for this process. In TEL–SYK mice, the SYK kinase is completely deregulated and consitutively activated within the cytoplasm, and its expression results in accumulation of immature and dysplastic megakaryoblasts in clusters in the BM. The mice develop a severe thrombopenia, showing the dysfunctionality of those cells. Dysplastic megakaryocytes are known to produce factors like platelet-derived growth factor[53,54] or transforming growth factor-β,[55–57] which are both potent stimulators of fibroblast proliferation and can contribute to myelofibrosis development, which is also seen in TEL–SYK mice. The fact that only 3 weeks are sufficient to cause a grade II–III myelofibrosis makes the TEL–SYK mouse model extremely interesting to identify further factors and cell types inducing or contributing to myelofibrosis and to test treatment strategies.

Previous publications found constitutive activation of SYK in AML induced by β2 integrins stimulated by factors coming from the BM niche and not by cell intrinsic oncogenes.[5] In line with those findings, SYK inhibition in AML/MPN cell lines effectively induced apoptosis and reduced proliferation, even in the presence of other oncogenic driver mutations. For example, the cell line SET-2 is derived from a patient with megakaryocytic leukemia after essential thrombocytosis and has an activated Jak2V617F mutation. Despite the known dependence of this cell line on oncogenic JAK2, the SYK inhibitor R406 was highly effective in inducing apoptosis, reduced proliferation and even blocked STAT5 signaling in those cells, pointing towards megakaryocytic leukemias as susceptable towards SYK inhibition even in the presence of JAK2V617F.

STAT5 is known to be a major driver of myeloproliferative diseases and is regulated by JAK kinases.[58,59] Previous publications have shown that SYK can directly interact with STAT5 and STAT3 in AML cell lines and can activate both proteins.[5] In our hands, we could not detect STAT3 activation by our SYK oncogenes, but in all our in vivo and in vitro models, we found activation of STAT5 by SYK kinases as the converging event. Furthermore, in SET-2 cells, STAT5 dephosphorylation was the sole phosphorylation event influenced by the SYK inhibitor treatment. Furthermore, the targeted deletion of STAT5 could completely block leukemia development and also myelofibrosis otherwise caused by TEL–SYK, strongly supporting the role of STAT5 as the major mediator downstream of the SYK kinase. As STAT5 is known to be deregulated in many myeloid malignancies, SYK inhibitors might be a highly interesting target in influencing STAT5 activity downstream of the classical oncogenes like JAK2V617F, BCR–ABL or various AML oncogenes, especially in situations where resistance occurs against the primary target. Furthermore, our results strongly support the use of SYK inhibitors in megakaryocytic leukemias and also in myelofibrosis patients and can pave the way towards a clinical trial in this patient cohort.

CONFLICT OF INTEREST

The authors declare no conflict of interest.

16

AUTHOR CONTRIBUTIONS

CS, HM, DB, TAM, JH, SK and JA performed the experiments; CK established flow cytometry analysis of stem cell populations; DP performed gene expression analysis; CD, JD, TB and HJ designed the research; CD and CS wrote the manuscript. KA analyzed the histology slides.

REFERENCES

1 Turner M, Mee PJ, Costello PS, Williams O, Price AA, Duddy LP et al. Perinatal lethality and blocked B-cell development in mice lacking the tyrosine kinase Syk. Nature 1995; 378: 298–302.

2 Cheng AM, Rowley B, Pao W, Hayday A, Bolen JB, Pawson T. Syk tyrosine kinase required for mouse viability and B-cell development. Nature 1995; 378: 303–306.

3 Ozaki N, Suzuki S, Ishida M, Harada Y, Tanaka K, Sato Y et al. Syk-dependent signaling pathways in neutrophils and macrophages are indispensable in the pathogenesis of anti-collagen antibody-induced arthritis. Int Immunol 2012; 24: 539–550.

4 Chan AC, van Oers NS, Tran A, Turka L, Law CL, Ryan JC et al. Differential expression of ZAP-70 and Syk protein tyrosine kinases, and the role of this family of protein tyrosine kinases in TCR signaling. J Immunol 1994; 152: 4758–4766.

5 Oellerich T, Oellerich MF, Engelke M, Munch S, Mohr S, Nimz M et al. beta2 integrin-derived signals induce cell survival and proliferation of AML blasts by activating a Syk/STAT signaling axis. Blood 2013; 121: 3889–3899.

6 Latour S, Fournel M, Veillette A. Regulation of T-cell antigen receptor signalling by Syk tyrosine protein kinase. Mol Cell Biol 1997; 17: 4434–4441.

7 Thome M, Duplay P, Guttinger M, Acuto O. Syk and ZAP-70 mediate recruitment of p56lck/CD4 to the activated T cell receptor/CD3/zeta complex. J Exp Med 1995; 181: 1997–2006.

8 Kulathu Y, Grothe G, Reth M. Autoinhibition and adapter function of Syk. Immunol Rev 2009; 232: 286–299.

9 Costello PS, Turner M, Walters AE, Cunningham CN, Bauer PH, Downward J et al. Critical role for the tyrosine kinase Syk in signalling through the high affinity IgE receptor of mast cells. Oncogene 1996; 13: 2595–2605.

10 Minami Y, Nakagawa Y, Kawahara A, Miyazaki T, Sada K, Yamamura H et al. Protein tyrosine kinase Syk is associated with and activated by the IL-2 receptor: possible link with the c-myc induction pathway. Immunity 1995; 2: 89–100.

11 Yousefi S, Hoessli DC, Blaser K, Mills GB, Simon HU. Requirement of Lyn and Syk tyrosine kinases for the prevention of apoptosis by cytokines in human eosinophils. J Exp Med 1996; 183: 1407–1414.

12 Hida S, Yamasaki S, Sakamoto Y, Takamoto M, Obata K, Takai T et al. Fc receptor gamma-chain, a constitutive component of the IL-3 receptor, is required for IL-3-induced IL-4 production in basophils. Nat Immunol 2009; 10: 214–222.

13 Buchner M, Baer C, Prinz G, Dierks C, Burger M, Zenz T et al. Spleen tyrosine kinase inhibition prevents chemokine- and integrin-mediated stromal protective effects in chronic lymphocytic leukemia. Blood 2010; 115: 4497–4506.

14 Gao J, Zoller KE, Ginsberg MH, Brugge JS, Shattil SJ. Regulation of the pp72syk protein tyrosine kinase by platelet integrin alpha IIb beta 3. EMBO J 1997; 16: 6414–6425.

15 Bu JY, Shaw AS, Chan AC. Analysis of the interaction of ZAP-70 and syk protein-tyrosine kinases with the T-cell antigen receptor by plasmon resonance. Proc Natl Acad Sci USA 1995; 92: 5106–5110.

16 Cornall RJ, Cheng AM, Pawson T, Goodnow CC. Role of Syk in B-cell development and antigen-receptor signaling. Proc Natl Acad Sci USA 2000; 97: 1713–1718.

17 Sada K, Takano T, Yanagi S, Yamamura H. Structure and function of Syk protein-tyrosine kinase. J Biochem 2001; 130: 177–186.

18 Deindl S, Kadlecek TA, Brdicka T, Cao X, Weiss A, Kuriyan J. Structural basis for the inhibition of tyrosine kinase activity of ZAP-70. Cell 2007; 129: 735–746.

19 Kulathu Y, Hobeika E, Turchinovich G, Reth M. The kinase Syk as an adaptor controlling sustained calcium signalling and B-cell development. EMBO J 2008; 27: 1333–1344.

20 Beitz LO, Fruman DA, Kurosaki T, Cantley LC, Scharenberg AM. SYK is upstream of phosphoinositide 3-kinase in B cell receptor signaling. J Biol Chem 1999; 274: 32662–32666.

21 Moon KD, Post CB, Durden DL, Zhou Q, De P, Harrison ML et al. Molecular basis for a direct interaction between the Syk protein-tyrosine kinase and phosphoinositide 3-kinase. J Biol Chem 2005; 280: 1543–1551.

22 Wienands J, Schweikert J, Wollscheid B, Jumaa H, Nielsen PJ, Reth M. SLP-65: a new signaling component in B lymphocytes which requires expression of the antigen receptor for phosphorylation. J Exp Med 1998; 188: 791–795.

23 Chiu CW, Dalton M, Ishiai M, Kurosaki T, Chan AC. BLNK: molecular scaffolding through 'cis'-mediated organization of signaling proteins. Embo J 2002; 21: 6461–6472.

24 Deckert M, Tartare-Deckert S, Couture C, Mustelin T, Altman A. Functional and physical interactions of Syk family kinases with the Vav proto-oncogene product. Immunity 1996; 5: 591–604.

25 Law CL, Chandran KA, Sidorenko SP, Clark EA. Phospholipase C-gamma1 interacts with conserved phosphotyrosyl residues in the linker region of Syk and is a substrate for Syk. Mol Cell Biol 1996; 16: 1305–1315.

26 Gururajan M, Jennings CD, Bondada S. Cutting edge: constitutive B cell receptor signaling is critical for basal growth of B lymphoma. J Immunol 2006; 176: 5715–5719.

27 Chen L, Monti S, Juszczynski P, Daley J, Chen W, Witzig TE et al. SYK-dependent tonic B-cell receptor signaling is a rational treatment target in diffuse large B-cell lymphoma. Blood 2008; 111: 2230–2237.

28 Carsetti L, Laurenti L, Gobessi S, Longo PG, Leone G, Efremov DG. Phosphorylation of the activation loop tyrosines is required for sustained Syk signaling and growth factor-independent B-cell proliferation. Cell Signal 2009; 21: 1187–1194.

29 Buchner M, Fuchs S, Prinz G, Pfeifer D, Bartholome K, Burger M et al. Spleen tyrosine kinase is overexpressed and represents a potential therapeutic target in chronic lymphocytic leukemia. Cancer Res 2009; 69: 5424–5432.

30 Duhren-von Minden M, Ubelhart R, Schneider D, Wossning T, Bach MP, Buchner M et al. Chronic lymphocytic leukaemia is driven by antigen-independent cell-autonomous signalling. Nature 2012; 489: 309–312.

31 Hahn CK, Berchuck JE, Ross KN, Kakoza RM, Clauser K, Schinzel AC et al. Proteomic and genetic approaches identify Syk as an AML target. Cancer Cell 2009; 16: 281–294.

32 Streubel B, Vinatzer U, Willheim M, Raderer M, Chott A. Novel t(5;9)(q33;q22) fuses ITK to SYK in unspecified peripheral T-cell lymphoma. Leukemia 2006; 20: 313–318.

33 Dierks C, Adrian F, Fisch P, Ma H, Maurer H, Herchenbach D et al. The ITK-SYK fusion oncogene induces a T-cell lymphoproliferative disease in mice mimicking human disease. Cancer Res 2010; 70: 6193–6204.

34 Pechloff K, Holch J, Ferch U, Schweneker M, Brunner K, Kremer M et al. The fusion kinase ITK-SYK mimics a T cell receptor signal and drives oncogenesis in conditional mouse models of peripheral T cell lymphoma. J Exp Med 2010; 207: 1031–1044.

35 Kuno Y, Abe A, Emi N, Iida M, Yamamori T, Tanimoto M et al. An atypical myelodysplastic syndrome with t(9;12)(q22;p12) and TEL gene rearrangement. Br J Haematol 1999; 106: 570–571.

36 Kanie T, Abe A, Matsuda T, Kuno Y, Towatari M, Yamamoto T et al. TEL-Syk fusion constitutively activates PI3-K/Akt, MAPK and JAK2-independent STAT5 signal pathways. Leukemia 2004; 18: 548–555.

37 Kuno Y, Abe A, Emi N, Iida M, Yokozawa T, Towatari M et al. Constitutive kinase activation of the TEL-Syk fusion gene in myelodysplastic syndrome with t(9;12)(q22;p12). Blood 2001; 97: 1050–1055.

38 Wossning T, Herzog S, Kohler F, Meixlsperger S, Kulathu Y, Mittler G et al. Deregulated Syk inhibits differentiation and induces growth factor-independent proliferation of pre-B cells. J Exp Med 2006; 203: 2829–2840.

39 Graham MT, Abram CL, Hu Y, Lowell CA. Expression of the TEL-Syk Fusion Protein in Hematopoietic Stem Cells Leads to Rapidly Fatal Myelofibrosis in Mice. PLoS One 2013; 8: e77542.

40 Cui Y, Riedlinger G, Miyoshi K, Tang W, Li C, Deng CX et al. Inactivation of Stat5 in mouse mammary epithelium during pregnancy reveals distinct functions in cell proliferation, survival, and differentiation. Mol Cell Biol 2004; 24: 8037–8047.

41 Hoelbl A, Schuster C, Kovacic B, Zhu B, Wickre M, Hoelzl MA et al. Stat5 is indispensable for the maintenance of bcr/abl-positive leukaemia. EMBO Mol Med 2010; 2: 98–110.

42 Pear WS, Miller JP, Xu L, Pui JC, Soffer B, Quackenbush RC et al. Efficient and rapid induction of a chronic myelogenous leukemia-like myeloproliferative disease in mice receiving P210 bcr/abl-transduced bone marrow. Blood 1998; 92: 3780–3792.

43 Ogata H, Goto S, Sato K, Fujibuchi W, Bono H, Kanehisa .. KEGG: Kyoto Encyclopedia of Genes and Genomes. Nucleic Acids Res 1999; 27: 29–34.

44 Kogan SC, Ward JM, Anver MR, Berman JJ, Brayton C, Cardiff RD et al. Bethesda proposals for classification of nonlymphoid hematopoietic neoplasms in mice. Blood 2002; 100: 238–245.

45 Lagresle-Peyrou C, Six EM, Picard C, Rieux-Laucat F, Michel V, Ditadi A et al. Human adenylate kinase 2 deficiency causes a profound haematopoietic defect associated with sensorineural deafness. Nat Genet 2009; 41: 106–111.

46 Rinaldi A, Kwee I, Taborelli M, Largo C, Uccella S, Martin V et al. Genomic and expression profiling identifies the B-cell associated tyrosine kinase Syk as a possible therapeutic target in mantle cell lymphoma. Br J Haematol 2006; 132: 303–316.

47 Lannutti BJ, Shim MH, Blake N, Reems JA, Drachman JG. Identification and activation of Src family kinases in primary megakaryocytes. Exp Hematol 2003; 31: 1268–1274.

48 Mazharian A, Thomas SG, Dhanjal TS, Buckley CD, Watson SP. Critical role of Src-Syk-PLC{gamma}2 signaling in megakaryocyte migration and thrombopoiesis. Blood 2010; 116: 793–800.

49 Ginsberg MH, Partridge A, Shattil SJ. Integrin regulation. Curr Opin Cell Biol 2005; 17: 509–516.

50 Shattil SJ, Newman PJ. Integrins: dynamic scaffolds for adhesion and signaling in platelets. Blood 2004; 104: 1606–1615.

51 Shattil SJ. Integrins and Src: dynamic duo of adhesion signaling. Trends Cell Biol 2005; 15: 399–403.

52 Obergfell A, Eto K, Mocsai A, Buensuceso C, Moores SL, Brugge JS et al. Coordinate interactions of Csk, Src, and Syk kinases with [alpha]IIb[beta]3 initiate integrin signaling to the cytoskeleton. J Cell Biol 2002; 157: 265–275.

53 Groopman JE. The pathogenesis of myelofibrosis in myeloproliferative disorders. Ann Intern Med 1980; 92: 857–858.

54 McCarthy DM. Annotation. Fibrosis of the bone marrow: content and causes. Br J Haematol 1985; 59: 1–7.

55 Martyre MC, Romquin N, Le Bousse-Kerdiles MC, Chevillard S, Benyahia B, Dupriez B et al. Transforming growth factor-beta and megakaryocytes in the pathogenesis of idiopathic myelofibrosis. Br J Haematol 1994; 88: 9–16.

56 Chagraoui H, Komura E, Tulliez M, Giraudier S, Vainchenker W, Wendling F. Prominent role of TGF-beta 1 in thrombopoietin-induced myelofibrosis in mice. Blood 2002; 100: 3495–3503.

57 Shehata M, Schwarzmeier JD, Hilgarth M, Hubmann R, Duechler M, Gisslinger H. TGF-beta1 induces bone marrow reticulin fibrosis in hairy cell leukemia. J Clin Invest 2004; 113: 676–685.

58 Kisseleva T, Bhattacharya S, Braunstein J, Schindler CW. Signaling through the JAK/STAT pathway, recent advances and future challenges. Gene 2002; 285: 1–24.

59 Ihle JN, Gilliland DG. Jak2: normal function and role in hematopoietic disorders. Curr Opin Genet Dev 2007; 17: 8–14.

Supplementary Information accompanies this paper on Blood Cancer Journal website (http://www.nature.com/bcj)